Tunable cell-surface mimetics as engineered cell substrates

Kent Shilts[a] and Christoph A. Naumann[a,b]

a. Department of Chemistry and Chemical Biology, Indiana University-Purdue University, Indianapolis, 46202 USA
b. Integrated Nanosystems Development Institute, IUPUI, Indianapolis, IN, USA

Summary:

Most recent breakthroughs in understanding cell adhesion, cell migration, and cellular mechanosensitivity have been made possible by the development of engineered cell substrates of well-defined surface properties. Traditionally, these substrates mimic the extracellular matrix (ECM) environment by the use of ligand-functionalized polymeric gels of adjustable stiffness. However, such ECM mimetics are limited in their ability to replicate the rich dynamics found at cell-cell contacts. This review focuses on the application of cell surface mimetics, which are better suited for the analysis of cell adhesion, cell migration, and cellular mechanosensitivity across cell-cell interfaces. Functionalized supported lipid bilayer systems were first introduced as biomembrane-mimicking substrates to study processes of adhesion maturation during adhesion of functionalized vesicles (cell-free assay) and plated cells. However, while able to capture adhesion processes, the fluid lipid bilayer of such a relatively simple planar model membrane prevents adhering cells from transducing contractile forces to the underlying solid, making studies of cell migration and cellular mechanosensitivity largely impractical. Therefore, the main focus of this review is on polymer-tethered lipid bilayer architectures as biomembrane-mimicking cell substrate. Unlike supported lipid bilayers, these polymer-lipid composite materials enable the free assembly of linkers into linker clusters at cellular contacts without hindering cell spreading and migration and allow the controlled regulation of mechanical properties, enabling studies of cellular mechanosensitivity. The various polymer-tethered lipid bilayer architectures and their complementary properties as cell substrates are discussed.

Table of Contents

This is the author's manuscript of the article published in final edited form as:

Shilts, K., & Naumann, C. A. (2018). Tunable cell-surface mimetics as engineered cell substrates. Biochimica et Biophysica Acta (BBA) - Biomembranes. https://doi.org/10.1016/j.bbamem.2018.06.009

1. Introduction

It is now widely recognized that fate and function of anchorage-dependent cells are influenced by a variety of different environmental cues including those of biochemical and mechanical origin. Cellular adhesions, such as integrin-based focal adhesions (FAs) or cadherin-based adherens junctions (AJs), play an important role in cellular mechanosensitivity [1, 2]. Not only being important sites of cellular force transduction during cell spreading and migration, they also serve as sophisticated environmental sensors of remarkable plasticity, which adapt their size, shape, composition, and density in response to external cues [3-7]. During this highly dynamic process, maturing cellular adhesions cluster together cell adhesion proteins and form stable linkages to the cytoskeleton [4, 8-13], enabling migrating cells to transmit cytoskeleton-generated forces to the surrounding environment [14-20]. Migrating cells not only probe the mechanical properties of the surrounding matrix by imposing cytoskeleton-generated traction forces and sensing the resulting mechanical responses, but also translate these mechanical cues into specific biochemical responses through a process known as mechanotransduction [21-27]. Notably, there is a correlation between malfunctions of cellular mechanotransduction and disease [28-31].

Previous advancements in the understanding of cellular mechanosensitivity have been closely linked to the development of engineered cell substrates of adjustable viscoelasticity, which allow a direct correlation between substrate stiffness and cell response. So far, this strategy has been mainly demonstrated on linker-functionalized polymeric gels, whose substrate elasticity can be controlled through polymer crosslinking density. Such polymeric substrates have been instrumental in confirming that substrate stiffness significantly impacts cellular

properties including morphology, cytoskeletal organization, and motility [32-37]. Most prominently, the significance of cellular mechanosensitivity was demonstrated by the observation that stem cell differentiation can be regulated by substrate stiffness [38]. Initial progress was made using artificial polymers, such as PAA [32], whereas later cellular mechanosensing experiments also included natural polymers of adjustable viscoelastic properties [39, 40]. Meanwhile, polymeric materials were also employed, which allow adjustment of substrate viscosity [41, 42]. In another ECM mimetic approach, cell adsorption was investigated on a cell substrate of amphiphilic peptides with RGD linkers [43].

While linker-functionalized polymeric gels can be considered as attractive ECM mimetics, they are usually limited in their ability to replicate the rich dynamics at cell-cell junctions, which include remarkable long-range movements, such as the observed basal-to-apical flow and treadmilling movements of AJs between polarized cells [44, 45]. Instead, alternative design strategies were needed in order to develop a more realistic cell surface-mimicking substrate for the analysis of cell adhesion and cell migration across cell-cell interfaces. As Fig. 1 illustrates, such a substrate should fulfill several important requirements. First, to enable cell adhesion and spreading on a cell surface mimetic, substrate-bound ligands for cell adhesion receptors should be able to dynamically assemble into clusters to allow the formation and maturation of stable cell-substrate linkages. Next, engineered cell surface mimetics for the analysis of cell migration should enable the transmission of cytoskeleton-generated cellular traction forces to the underlying solid substrate across cell-substrate attachments. Finally, such artificial cell substrates should permit the adjustment of substrate mechanical properties to make them suitable for the characterization of cellular mechanosensitivity.

The current review focuses on the design and application of cell surface mimetics for the analysis of cell adhesion, cell migration, and cellular mechanosensitivity. Chapter 2 discusses the design and previous applications of supported lipid bilayer (SLB) systems as artificial substrates for the study of cell adhesion processes. These biomembrane mimetics are particularly useful as *in vitro* experimental platform for investigating cell adhesion processes under well-defined substrate conditions. Specifically, Chapter 2.1 focuses on the fabrication and characterization of SLBs. Chapter 2.2 gives an overview of previous developments in cell-free assays, which provided valuable insight into the underlying biophysical mechanisms of cell adhesion. As discussed in Chapter 2.3, ligand-functionalized SLBs have also been applied to explore the process of artificial immunological synapse formation upon adhesion of immune cells. Because the topic of SLBs as model membranes and biomembrane-mimicking cell substrates has been reviewed previously [46-48] and because such relatively simple cell surface mimetics do not allow development of cellular traction forces required in cell migration and cellular mechanosensing, the particular emphasis of the current review is on the design and application of polymer-tethered lipid bilayer (PTLB) architectures as cell surface mimetics for the analysis of cell migration and cellular mechanosensitivity (Chapter 3). PTLBs have previously been introduced as a model membrane system for the analysis of membrane proteins [49-51]. As outlined in this review, PTLBs also represent an attractive model membrane architecture, which overcomes the limitations of SLB as artificial cell substrate. Comparable to SLB, PTLB enable the dynamic arrangement of ligands on its surface to form stable linkages with adhering cells. However, unlike SLBs, PTLB architectures do not suppress cellular tractions, making them a suitable experimental platform for the analysis of cell migration. Chapter 3.1 describes the different fabrication methods of PTLBs. Chapter 3.2 provides previous results of PTLB characterization. This chapter demonstrates that adjustment of polymer-tethered lipids not only

allows variation of bilayer fluidity (Chapter 3.2.1), but also enables controlled modification of substrate mechanical properties (Chapter 3.2.2), making studies of cellular mechanosensitivity feasible. Chapter 3.3 discusses previous applications of PTLBs as cell-surface mimicking substrates to study cell spreading/migration and cellular mechanosensitivity (Chapter 3.4). Chapter 4 gives a conclusion and outlook.

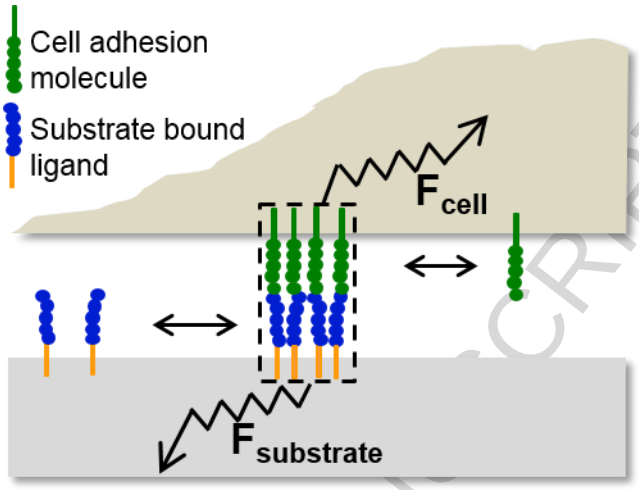

Fig. 1: Schematic illustrating the functionality of an advanced cell surface-mimicking cell substrate, which allows: (i) dynamic assembly of linkers into linker clusters at cell-substrate contacts, shown in dashed line; (ii) transduction of cytoskeletal forces through cell-substrate contacts to enable cell spreading and migration, shown with force vector; and (iii) dissipative long-range movements of cell-substrate contacts.

2. Solid-supported lipid bilayer as cell substrate

2.1. Fabrication and characterization of solid-supported lipid bilayer

Since introduction by McConnell and coworkers more than three decades ago, SLBs have developed into a widely employed model membrane platform for biophysical and biotechnological applications [47, 52, 53]. Formation of a planar lipid bilayer by roll out and fusion of unilamellar vesicles represents the most widely established SLB fabrication method [54]. Alternatively, a SLB can be built through monolayer transfer from the air-water interface [52] or via spreading from a lipid reservoir [55]. Importantly, physical interactions lead to an energy minimum that position the SLB ~10 Å above a hydrophilic solid substrate, separated by a thin water layer [56, 57]. Due to the resulting lubrication effect of the thin water layer, lipids in both leaflets and lipid-anchored proteins in the top leaflet of the SLB display lateral mobility, resembling an important property of plasma membranes [52]. In contrast, transmembrane proteins with a cytosolic domain are typically immobilized in such model membranes [58]. Like other lipid bilayer systems, SLBs have highly anisotropic mechanical properties. They show a liquid-like in-plane shear viscosity and a rather elastic response with respect to out-of-plane deformations [59, 60]. As discussed in the next two chapters, fluid SLBs have also emerged as a promising experimental platform for the analysis of adhesion processes of functionalized vesicles and plated cells, respectively.

2.2. Solid-supported lipid bilayer as cell surface mimetic in cell-free assay to study adhesion

In part, motivated by the classical model of Bell, Dembo, and Bongard that cell adhesion depends on the competition between specific and generic interactions [61], Sackmann and coworkers explored in a series of papers the biophysical aspects of cell adhesion by investigating the interaction between functionalized giant vesicles and SLBs. In this cell-free assay, giant vesicles are doped with glycocalix-mimicking lipopolymers, acting as repellers, and ligand molecules, which enable specific binding to reconstituted receptors in the SLB that may also contain lipopolymers (Fig. 2 panel on the left). A hallmark of such an assay is the ability of laterally mobile ligands, receptors, and repellers to dynamically rearrange during the adhesion process. This model system is attractive because both the ligand and receptor concentrations in the SLB and giant vesicles can be adjusted quite accurately. This feature enables the design of experiments, which provide insight into the role of receptor and ligand concentrations on the vesicle adhesion process. For example, the RICM data in Fig. 2 upper right show that systematic variation of contact site A (csA) ligand on the vesicle alters the contact zone between adhering vesicle and SLB [62]. Interestingly, at lower csA concentrations, domains of tight adhesion and weak adhesion can be observed underneath the adhering vesicle. Similarly, the fluorescence data in Fig. 2 bottom right demonstrate the ability to investigate the impact of a controlled receptor shortage on the vesicle adhesion process to a SLB [63]. They show that such a receptor shortage results in an adhesion zone of coexisting regions of tighter and weaker adhesion.

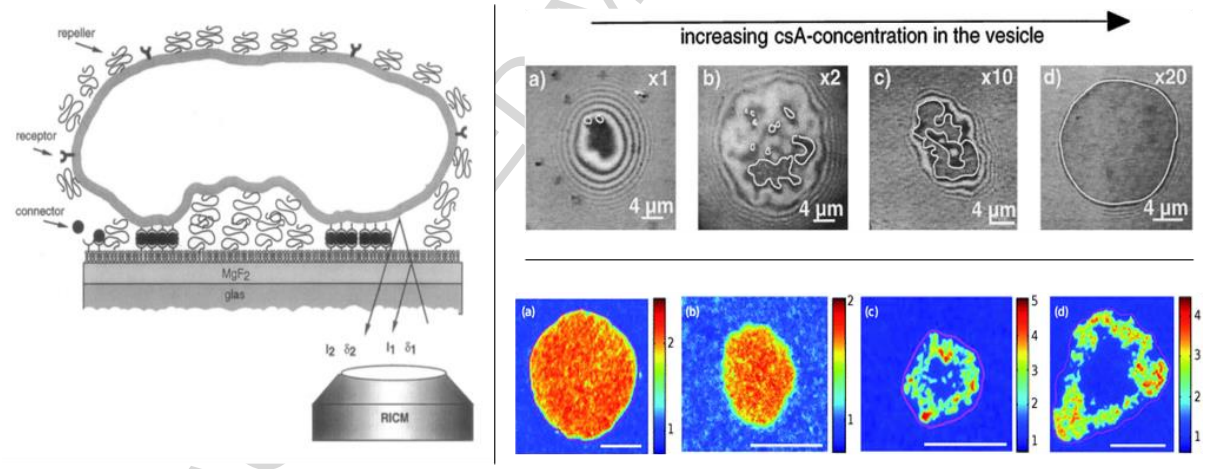

Fig. 2: Left panel: Schematic of a cell-free assay for the study of cell adhesion processes. Here, a giant vesicle is doped with glycocalix-mimicking lipopolymers, acting as repellers, and ligand molecules, which enable specific binding to reconstituted receptors in the SLB. The adsorption process can be monitored using microscopic techniques, such as reflection interference contrast microscopy (RICM). Top right: RICM data illustrate the impact of csA ligand concentration in the vesicle on the vesicle adsorption to a csA-functionalized SLB. Fluorescence microscopy methods (bottom right) may provide important insight into the subtle interplay between ligand-receptor pairs if ligands and/or receptors are fluorescently labeled. Left panel [64], top right [62], and bottom right [63] reprinted with permission from publishers.

Previously, adhesion experiments with this cell-free assay were conducted using different ligand-receptor pairs, including heterophilic biotin-streptavidin [64] and RGD-$\alpha_{IIb}\beta_3$ integrin [65], as well as homophilically binding contact site A (csA) receptors [62]. These experiments showed that low receptor concentrations can trigger the adhesion process between giant vesicle and SLB by forming tightly binding adhesion domains of ligand-receptor pair clusters, thereby displaying remarkable parallels to the assembly of adhesion proteins at cellular contacts [66]. The observed ligand-receptor segregation was described by a double minimum free energy of adhesion and was interpreted in terms of a competition between short-range attractive forces and long-range repulsive forces. By combining the described cell-free assay with a magnetic tweezer setup, Sackmann and coworkers also demonstrated force-induced adhesion strengthening in such a model system [67]. Smith and coworkers, using a cell-free adhesion assay with cadherin receptors, also reported that membrane fluctuations may have a significant impact on adhesion processes between functionalized giant vesicles and SLBs [68]. Taken together, the described experiments not only established the significance of specific key-lock binding processes during giant vesicle adhesion to the SLB, but also illustrated the importance of physical interactions in the adhesion process. Interestingly, Parthasarathy and Groves also reported that adhesion of ligand-free vesicles without specific ligands may cause segregation of SLB-bound proteins into micron-size clusters [69].

2.3. Solid-supported lipid bilayers (SLBs) as an artificial cell substrate

In addition to cell-free adhesion assays, SLBs of well-defined ligand composition have also been utilized as an *in vitro* experimental platform for investigating adhesion processes of plated cells. Most prominently, this experimental strategy was successfully applied in combination with immune cells to study artificial immunological synapse formation [70, 71]. McConnell and coworkers first reported the activation of CD8 positive T-cells on supported lipid membranes with incorporated major histocompatibility complex class I proteins [54]. By building on these pioneering experiments, the SLB platform was next applied to investigate the adhesion of lymphocytes to a supported lipid bilayer via heterophilic CD2/CD58 interaction [70]. These experiments not only identified the formation of ligand-receptor pairs, but also established the accumulation of laterally mobile CD58 at contact areas between Jurkat T lymphoblasts and SLB. Analysis of cellular adhesion processes was not limited to a CD58-containing SLB, but also included other ligands, such as ICAM-1 [72, 73]. Notably, in such experiments, CD58 and ICAM-1 in the planar bilayer were found to dynamically redistribute into segregated CD2-CD58 and LFA-1-ICAM-1 adhesions between SLB and adhering cell. This finding was significant because it illustrated that ligand-containing SLBs allow the dynamic rearrangement of adhesion proteins into distinct synaptic patterns underneath plated cells. As illustrated in Fig. 3, quantitative analysis of fluorescence data of fluorescently labeled ligands in such an *in vitro* assay demonstrated that immunological synapse formation goes through distinct stages, including junction formation (stage 1), MHC- peptide transport (stage 2), and synapse stabilization (stage 3) [74]. These findings were intriguing in light of the detected synaptic pattern formation between antigen-presenting cells and T-cells during T-cell activation [75]. They illustrate that SLB of well-defined ligand composition have become a valuable tool of immune cell adhesion/activation research [75, 76]. SLBs were also employed to explore molecular processes associated with artificial neuronal synapse formation [77] and to investigate the mechanobiology of nascent integrin and cadherin adhesions [78-80]. Furthermore, comparing

experiments on ligand-functionalized SLB versus control substrates with corresponding immobilized ligands allowed valuable insight into the role of ligand mobility during cell adhesion and activation. For example, cell adhesion experiments on SLBs revealed that ligand mobility may modulate artificial immunological synapse formation and activation of plated T-cells [81]. In this case a more rapid formation of the central supramolecular activation cluster as well as enhanced tyrosine phosphorylation and Ca^{2+} levels were seen as indicators of cell stimulation on SLBs with laterally mobile ligands. Similarly, the lateral mobility of E-cadherin in a SLB was reported to influence E-cadherin-mediated intracellular signaling in epithelial cells [82]. In the latter case, laterally mobile E-cadherin in the SLB was observed to enhance recruitment of the Rho GTPase family member Rac1(relative to immobilized E-cadherin) that plays important roles in downstream E-cadherin signaling and as an upstream effector of cytoskeletal dynamics influencing E-cadherin behavior [82]. Another noteworthy development has been the introduction of molecular tension sensors to probe cellular tensions during cellular adhesion to a SLB [46, 83, 84]. Specifically, molecular tension fluorescence microscopy (MTFM) sensors have been applied to measure cellular tensions on a SLB [83, 84]. These experiments demonstrated that the presence of the planar model membrane leads to reduced cellular tensions relative to substrates with corresponding immobilized tension sensors. For example, T-cells showed a cellular tension of 4.7 pN on a SLB [83], but were able to open immobilized 12 pN tension gauge tethers [85]. Similar results were obtained using B-cells, which showed unzipping of 7 pN sensors but no unzipping of 9 pN and 14 pN probes on SLB [84], whereas a 56 pN tension probe was opened on a glass substrate [86].

Despite their suitability in deciphering processes of immunological synapse formation and nascent cellular adhesion formation, SLBs have been limited in their applicability as an artificial cell substrate because adhering cells are typically unable to develop cellular tractions on a fluid SLB of negligible shear viscosity. Consequently, such a fluid bilayer system may allow the formation of nascent adhesion structures, but suppresses the development of matured cellular adhesions required in a process, such as cell migration [79]. To overcome this limitation, SLBs have been previously compartmentalized using lithographically patterned grids [87]. For example, MCF-7 cells were unable to spread on a planar fluid lipid bilayer with laterally mobile hEGF-linkers, but showed good spreading behavior on corresponding substrates with incorporated micropatterns of immobilized anchors [88]. SLBs with engineered micropatterns have also been employed to impose constraints on immunological synapse formation, resulting in altered TCR signaling [89]. A corresponding experimental strategy was applied to demonstrate that physical restriction of laterally mobile ephrin-A1 ligands in a patterned SLB impacts the organization and physical force sensing of EphA2 receptors in adhering breast cancer cells [90] . Another interesting example represents a SLB where neuronal adhesion protein was conjugated to an Fc-domain of IgG, thus enabling neuronal adhesion and growth [91]. An alternative patterning strategy has been the incorporation of surface-functionalized nanoparticles and nanodot arrays into SLBs, enabling the design of cell substrates with well-defined regions of immobilized and laterally mobile ligands [92, 93]. Such patterning strategies are also noteworthy because they provide some tunability in terms of substrate mechanical properties. Interestingly, Biswas et al. previously demonstrated the formation of stable AJ and cell spreading on a SLB without micropatterns [94]. In this case, the SLB contained lipids with a bulky dye moiety, resulting in a bilayer of higher viscosity. Their study was also notable because, unlike in the case of FAs, the presence of diffusion barriers in a fluid SLB was insufficient to result in the formation of AJs, indicating the significance of long-range

movements of cadherins during AJ formation [95]. Taken together, the described applications illustrate the significance and versatility of SLBs as an artificial cell substrate [77]. Moreover, it should be emphasized that key aspects of vesicle/cell adhesion on ligand-functionalized SLBs are also applicable to other cell surface mimetics with laterally mobile ligands, such as PTLBs (discussed in Chapter 3).

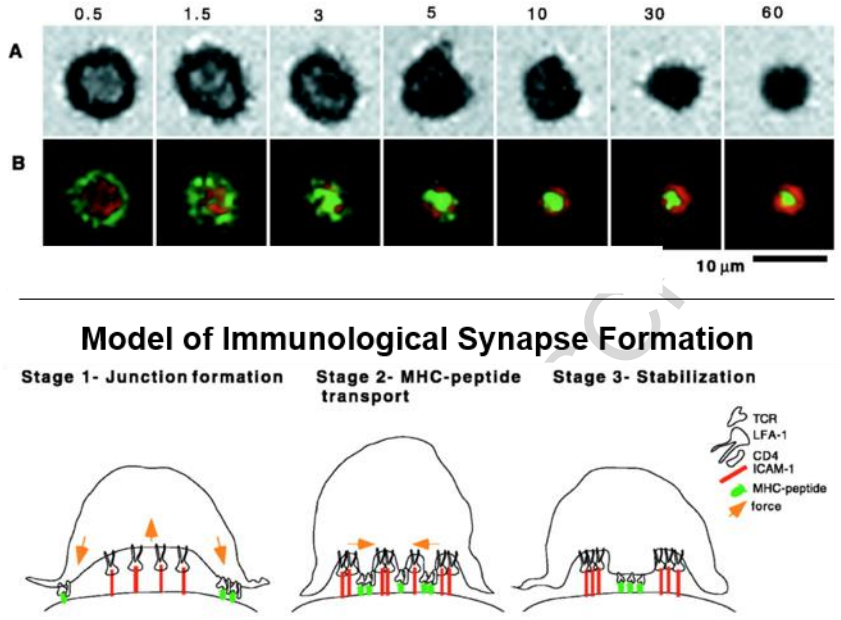

Fig. 3: Formation of immunological synapse, between 2B4 cells and SLB containing MHC-peptide and the adhesion ligand ICAM-1. Information about synapse formation can be obtained by acquiring images of contact formation (A) and distribution of fluorescently tagged MHC-peptide (green) and ICAM-1 (red) shown in (B). Model of immunological synapse formation, as derived from quantitative analysis of fluorescence data, shown in bottom panel. According to this model, immunological synapse formation goes through three stages: junction formation (stage 1), MHC- peptide transport (stage 2), and synapse stabilization (stage 3). Reprinted from [74] with permission from publisher.

3. Polymer-tethered lipid bilayers (PTLBs) as an artificial cell substrate

3.1. Fabrication of PTLB architectures

3.1.1. Fabrication of single PTLB

Polymer-supported lipid bilayers have been introduced to overcome the limitations of SLBs for the study of transmembrane proteins [49]. Their hallmark is the presence of a soft polymer layer underneath the lipid bilayer, causing the lift up of the bilayer from the underlying solid substrate. Depending on the type of fabrication method and polymer system used, the addition of the polymer layer can result in bilayer-substrate distances of 5-100 nm, making these model membranes suitable as experimental platforms for the analysis of transmembrane proteins. However, the assembly of polymer-supported membranes is usually more complex than the

previously described fabrication of SLBs. In fact, great care should be taken in the selection of the polymer, lipid bilayer composition, and surface chemical properties of the solid substrate to build a thermodynamically stable polymer-supported lipid bilayer. One key requirement of a successful fabrication method is the ability of the selected polymeric material to form a continuous, defect-free thin film on the solid substrate proteins [49, 50]. Moreover, the surface properties of the polymer film should allow the reliable attachment of a lipid bilayer, resulting in a stable polymer-supported lipid bilayer system. In addition to these stability requirements, the chosen polymeric material should also fulfill other important functional roles. Most obviously, the polymer should be hydrophilic to maintain an aqueous reservoir between bilayer and solid substrate. Finally, it is beneficial to employ a polymer with chemically inert bulk properties to minimize unwanted perturbations on the functionality of reconstituted membrane proteins.

Previously, several different strategies of polymer-supported lipid bilayer assembly have been pursued [51]. One relatively straightforward fabrication approach relies on the application of polyelectrolytes as cushion material and the subsequent addition of a bilayer containing a certain fraction of lipids with oppositely charged headgroups [96, 97]. The attachment of the bilayer on the surface of polyelectrolytes using attractive electrostatic interactions can be combined with the established method of layer-by-layer deposition of polyelectrolytes, which provides flexibility in terms accessible polymer cushion thicknesses [98]. However, the presence of polyelectrolytes in electrostatically stabilized polymer-supported lipid bilayers may have a perturbing effect on the properties of reconstituted membrane proteins. Therefore, an alternative method has emerged: namely, the stable attachment of the lipid bilayer to the polymer cushion by tethering. The resulting supramolecular assembly, referred to as a PTLB, is attractive because polymers with inert bulk properties can be utilized and stable PTLB architectures can be built without substantially compromising bilayer fluidity. As outlined below, two main strategies of PTLB fabrication have been pursued.

In one strategy of PTLB fabrication (in the following referred to as "*bottom-up*" method), the polymeric material is spin-coated onto a pretreated solid substrate of well-defined surface chemistry. The polymer may contain reactive groups, which target functional groups on the substrate surface, guaranteeing formation of a stable polymer coating [99]. In a next step, a lipid monolayer is attached to the substrate with the functionalized polymer film using a Langmuir-Blodgett dipping process. In this case, stable attachment of the lipid layer to the polymer film is typically accomplished by functionalized lipids, which are tailored towards specific functional groups on the surface of the polymer film. Alternatively, the polymeric material may be functionalized with lipid-like anchors, which incorporate into the attached lipid monolayer following LB transfer [100, 101]. The polymer-supported lipid bilayer is completed either through vesicle fusion or monolayer transfer using the Langmuir-Schaefer technique. Notably, a similar fabrication strategy has been pursued by targeting functional groups on the polymer surface towards tagged membrane proteins, resulting in protein-tethered lipid bilayer systems [102, 103]. Alternatively, bilayer tethering was also achieved by targeting transmembrane peptides in the lipid bilayer [104]. Meanwhile, a variety of different polymeric materials have been reported as cushion materials, such as polyacrylamide, cellulose, agarose, and PEG [105].

The other main strategy of PTLB fabrication (referred to as "*top-down*" fabrication method) relies on the use of lipopolymers, which are lipid or lipid-like molecules with a macromolecular (typically polymeric) moiety, such as as PEG or poly(2-methyl-2-oxazoline). During a typical film assembly with these amphiphiles, a mixed monolayer of lipopolymers and phospholipids is transferred from the air-water interface to a solid substrate using the Langmuir-

Blodgett method. Again the bilayer can be completed using vesicle fusion or Langmuir-Schaefer lipid monolayer transfer [106, 107]. To maintain a stable linkage between lipopolymers and solid substrate, attachment of lipopolymers to glass substrates has been achieved through either lipopolymers with terminal silane groups [106, 108] or photocrosslinking between lipopolymers and benzophenone-silane-coated surfaces [107, 109]. Similarly, thiol coupling chemistry has been utilized to tether lipids to Au substrates [110, 111]. Stable PTLBs have also been built without chemical attachment to the solid substrate, resulting in physisorbed membrane systems [112].

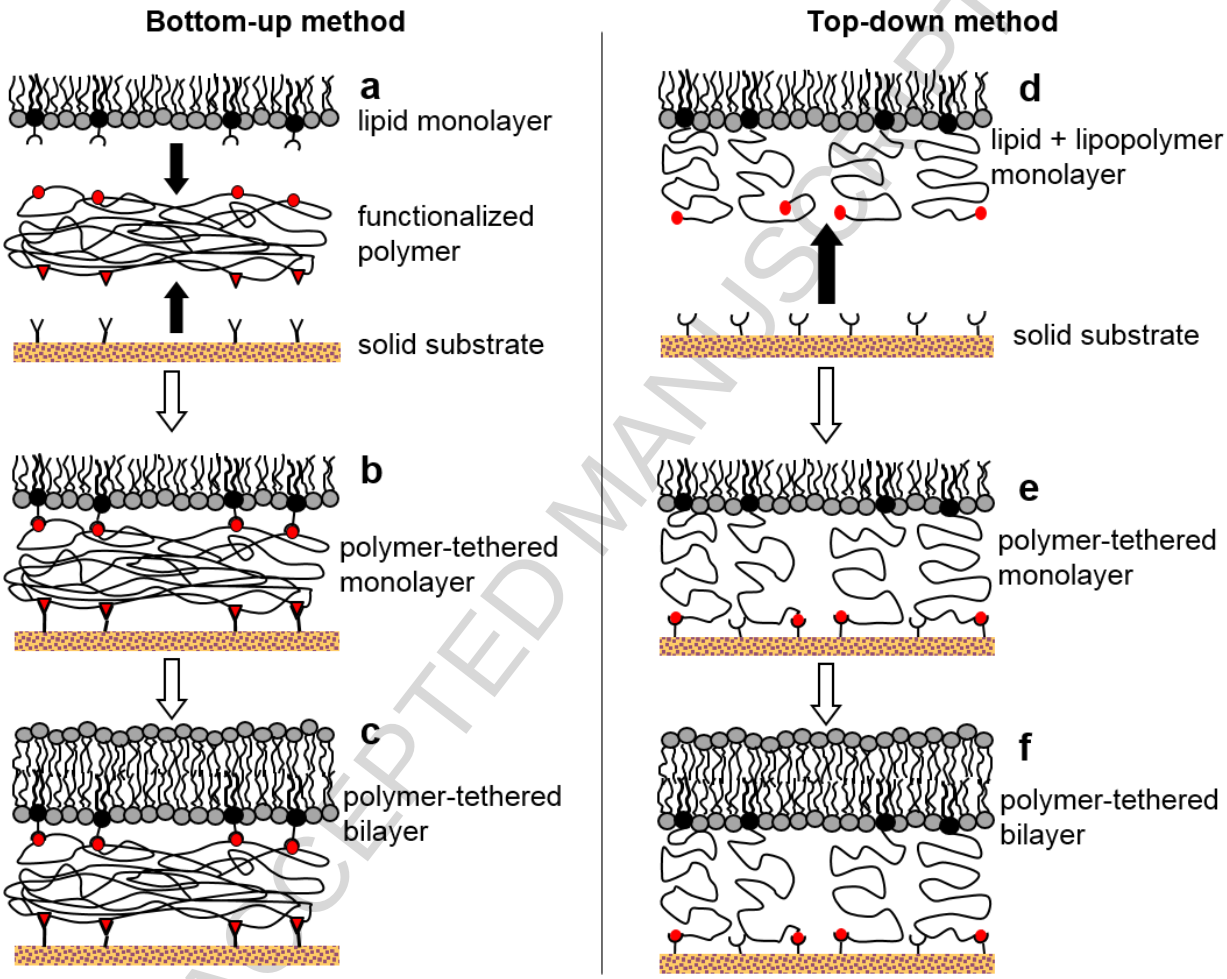

Fig. 4: Two distinct pathways of PTLB assembly (red shapes indicate covalent bonding). On the left, layer-by-layer assembly using the *bottom-up* fabrication method is shown, in (**a**) the solid substrate, polymer and lipid monolayer are formed separately; **b** the monolayer is linked to the polymer cushion and **c** the PTLB is completed. Covalent bonding can be utilized to stabilize interfaces between solid and polymer as well as polymer and lipid. On the right, assembly of a PTLB using the *top-down* method is shown: **d** the inclusion of lipid-polymer hybrid molecules allows a polymer-tethered monolayer to be fabricated in one step, **e** the monolayer can be covalently linked to the glass substrate and **f** the PTLB is completed.

The two described PTLB fabrication methods, *bottom-up* and *top-down*, are complementary in nature. As shown in Fig. 4, in the initially described *bottom-up* method, the properties of the membrane system are largely set by the properties of the functionalized polymer. Moreover, an accurate control of the tethering density between polymer and lipid bilayer remains challenging. In contrast, the *top-down* lipopolymer-based fabrication method allows the facile adjustment and control of membrane properties by regulating the molar concentration of lipopolymers in the proximal monolayer of the polymer-supported lipid bilayer. However, while this fabrication method allows a precise control of tethering density at the polymer-bilayer interface, it remains somewhat limited to a comparably thin polymeric cushion thickness of typically less than 10 nm. In contrast, spin-coated polymer cushions may in principle reach a thickness of hundreds of nm.

3.1.2. Fabrication of polymer-tethered lipid multi-bilayers

In addition to single PTLBs, polymer-tethered lipid multi-bilayers have emerged as an alternative planar model membrane platform. Multi-bilayer stacking provides a viable pathway for the fabrication of planar model membranes, which are less influenced by the underlying solid substrate than SLBs. Previously, several different approaches of supported lipid double bilayer formation have been reported. Kaizuka and Groves described the formation of double bilayers by fusing GUVs containing negatively charged glycolipids or anionic lipids, respectively, to a SLB containing cationic lipids [113]. Alternatively, double bilayer formation was accomplished by linking two lipid bilayers, which are partly comprised of cationic lipids and DNA duplexes, respectively [114], as well as through DNA hybridization [115]. However, in these cases, there were either uncertainties about the DNA orientation and associated inter-bilayer distance or the double bilayer system showed limited stability. In contrast, formation of a stable double bilayer system was achieved by using biotin-streptavidin or NHS/EDC coupling strategies [116, 117].

Our group previously reported an alternative approach of multi-bilayer fabrication [118]. In this case, a single PTLB containing phospholipids and lipopolymers was first assembled using the LB/LS method and additional bilayers were attached by addition of GUVs containing a portion of membrane constituents with either thiol or maleimide functional groups. This strategy allows the formation of stable inter-bilayer linkages in the polymer-tethered lipid multi-bilayer stack. Notably, the described multi-bilayer assembly method was not limited to the fabrication of a double bilayer system, but also included the assembly of stable stacks containing three and four bilayers. Here the layer-by-layer assembly can be considered conceptually similar to the assembly of polymer multilayers using oppositely charged polyelectrolytes [98]. Fluorescence microscopy demonstrated that bilayers within the stack are free of optically visible defects and show good stability (Fig. 5). They were found to be durable over a time period of at least 48 h. Complementary AFM experiments showed furthermore that the stacking of multiple bilayers also changes bilayer morphology, leading to less planar bilayers with increasing bilayer-substrate distance (Fig. 10c-d). Changes of morphology with bilayer number were also reported elsewhere [119]. AFM analysis also revealed the occasional formation of small, sub-optical resolution size bilayer defects, which presumably were caused by membrane-penetrating polymeric chains [120].

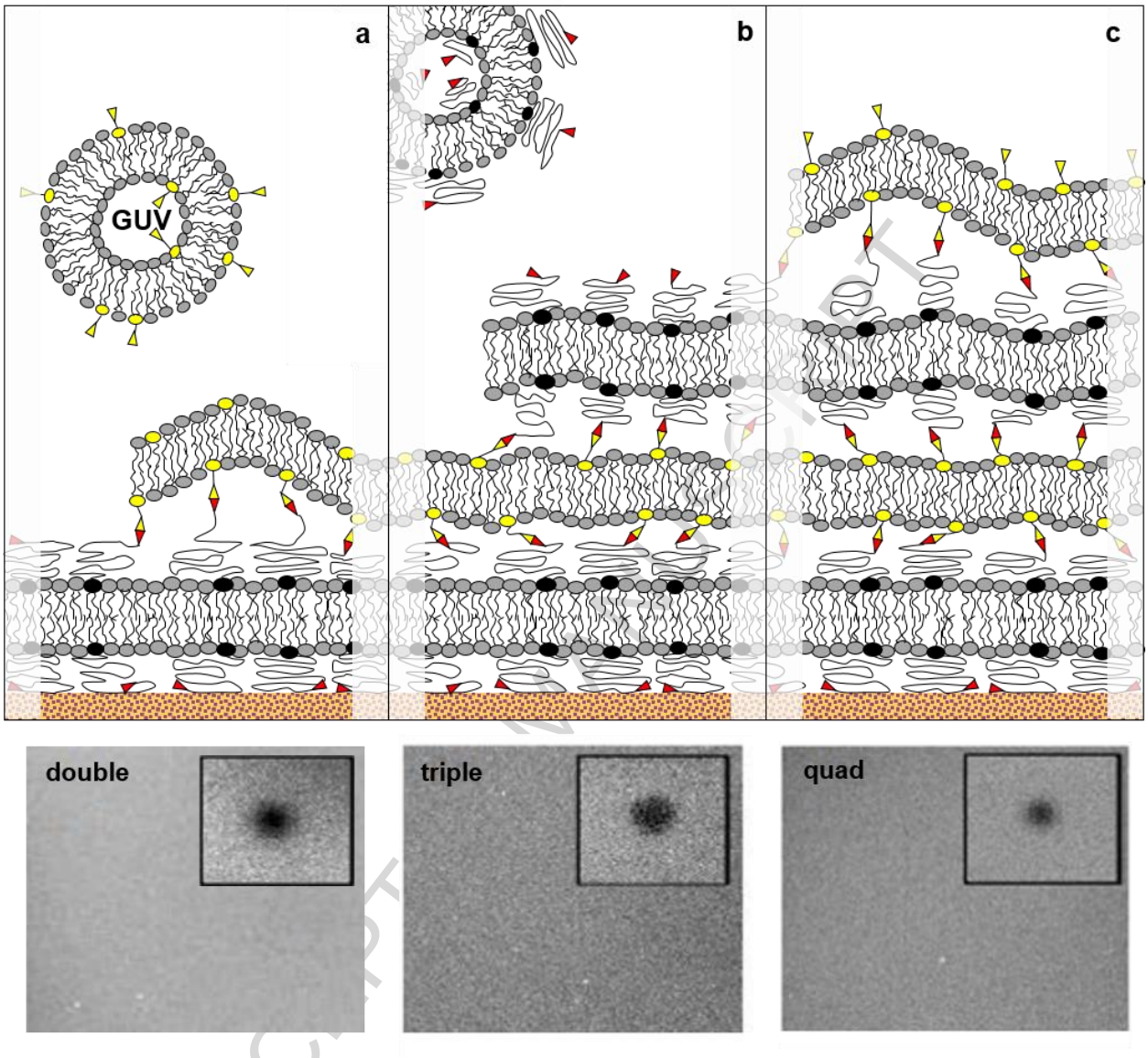

Fig. 5: Schematic showing assembly of polymer-tethered lipid multi-bilayer stack by fusion of functionalized giant unilamellar vesicles containing either SH-lipids (yellow) or PEG lipopolymers with a terminal maleimide group (red) into double (**a**), triple (**b**), and quadruple (**c**) bilayer systems. Fluorescence micrographs confirm the homogeneity of individual bilayers in the stack. Shape of bleaching spots in insets illustrate bilayer fluidity, dimensions of the micrographs are 90 µm x 90 µm for each image and insets in double and triple bilayers are 36 µm x 36 µm, inset in quadruple is 64 µm x 64 µm. Fluorescence micrographs were reprinted from [118] with permission from publisher.

3.1.3. Fabrication of PTLBs with lipopolymer pattern/gradient

It is well known that anchorage-dependent cells have a preference for a specific set of mechanical properties in the microenvironment. To explore properties of cellular mechanosensitivity, one attractive experimental strategy has been the development of cell motility assays using polymeric substrates with an elasticity gradient [36]. For example, various fabrication methods for the design of polymer thin films with gradients [121] and sharp boundaries in particular polymer properties [122, 123] have been reported. In contrast to polymeric films, traditional SLBs cannot be built with static elasticity gradients. An interesting exception represents a planar lipid bilayer, which contains heterogeneously distributed polymerizable lipids, resulting in a SLB with region-specific lipid diffusivity [124]. Another promising technology that can be applied to create patterned PTLBs represents the incorporation of nanopatterns of biomolecules using nanoparticle arrays [93].

Previously, patterning strategies have also been reported for PTLBs [125]. In one case, PTLBs have been built, which are characterized by a sharp boundary between regions of low (no buckling structures) and high (with buckling structures) lipopolymer concentrations (Fig. 6a). Such a patterned PTLBs can be accomplished by regulating the phospholipid-lipopolymer mixing ratio at the air-water interface and by conducting partial LB transfers at altered lipopolymer concentrations. In another patterning strategy, a lateral tethering (elasticity) gradient was achieved by regulating the phospholipid-lipopolymer mixing ratio at the air-water interface prior to LB transfer and by subsequent transfer of the polymer-tethered membrane to the solid (glass) substrate (Fig. 6b).

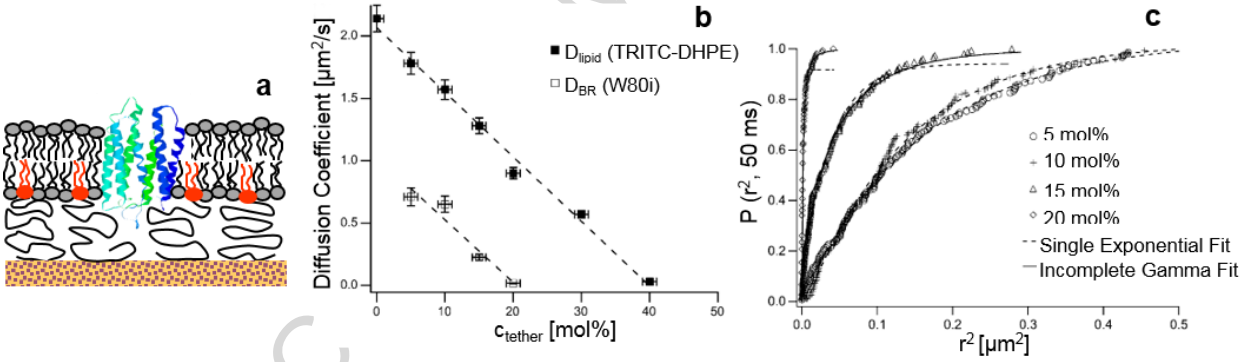

Fig. 6: Schematic of a physisorbed PTLB (**a**), which contains a well-defined concentration of lipopolymers in its inner leaflet. This model membrane architecture allows the incorporation of transmembrane proteins, such as bacteriorhodopsin. (**b**) Impact of lipopolymer molar concentrations, described by tether concentration, c_{tether}, on the lateral diffusion of phospholipids (TRITC- DHPE) and the monomeric bacteriorhodopsin mutant (W80i). (**c**) Cumulative distribution function analysis of single molecule tracking data shows Brownian lipid diffusion at lower lipopolymer concentration, but anomalous lipid diffusion at elevated tethering densities. Reprinted from [112] with permission from publisher.

As shown in Fig. 6a and b, membrane patterns can be visualized on the basis of membrane buckling structures at elevated lipopolymer concentrations. An attractive feature of such patterned substrates is that, due to the physisorption of lipopolymers at the glass surface,

resulting patterns and gradients of lipopolymers remain static. This allows the design of PTLBs with exciting properties, including gradual changes in length scale dependent lipid diffusivity and membrane elasticity. An important benefit of patterned PTLBs is the ability to modify a single parameter in a multivariate environment and to study the system's response to changes of this single parameter. Another interesting patterning strategy represents the controlled formation of stripe phases in polymer-tethered lipid bilayers comprised of lipids and lipopolymers, in which stripe formation was controlled through changing LB transfer conditions [126].

In addition to the above described patterning methods, patterning strategies, developed for SLB, should also be applicable to PTLB. In particular to *bottom-up* fabrication method of PTLB should it make feasible to build compartmentalized PTLB on substrates with engineered patterned grids using photoresist, aluminium oxide, or gold on oxidized silicon substrates [87, 127, 128] This capability was previously demonstrated by Waichman et al. who showed that the technique of creating patterned membranes can be extended to polymer-supported systems. [129]. They employed their patterned substrate to create membrane corrals, in which diffusion properties of individual transmembrane receptors could be studied [129].

3.2. Characterization of PTLB systems

3.2.1. Structural Characterization of PTLBs

As outlined in Chapter 3.1.1, great care should be taken in the fabrication of PTLB systems as their assembly depends on several parameters, such as bilayer composition, polymer cushion properties, and surface chemical properties of the solid substrate. Therefore, it has been important to test the structure and organization of PTLB upon the assembly process.

Our group previously confirmed the presence of the polymer cushion between bilayer and glass substrate in a physisorbed PTLB comprised of SOPC and the lipopolymer [dioctadecylamine [poly(2-ethyl-2-oxazoline) 8988] (DODA-E85) by comparing single molecule diffusion data of TAMRA-labeled lipopolymers in the bottom and top leaflets of the PTLB system [130]. As expected the lateral diffusion of 5 and 10 mol% dye-labeled lipopolymers in the bottom monolayer was about two orders of magnitude lower than that of dye labeled lipids in the same leaflet of the bilayer. In contrast, dye-labeled lipopolymers and dye-labeled lipids displayed comparable lateral diffusivity in the top leaflet of this physisorbed PTLB system. In agreement with our experimental findings, Watkins et al. reported neutron and X-ray reflectivity, which support the formation of a physisorbed polymer-tethered lipid monolayer containing PEG lipopolymers [131]. However, these authors did not observe a stable physisorbed polymer cushion upon Langmuir-Schaefer deposition of the second monolayer. Only after usage of lipopolymers with reactive terminal groups, which are able to bind covalently to the glass substrate, a polymer-cushioned bilayer system could be observed that showed a bimodal distribution of cushioned and cushion-free bilayer regions.

One attractive feature of polymer-cushioned bilayers represents the ability of the controlled uplift of the bilayer from the underlying solid substrate. For example, fluorescence interference microscopy studies demonstrated that the polymer conformations of PEG lipopolymers in a PTLB are well described by scaling laws of polymer physics [132]. Specifically, the cushion thickness for low concentrations of lipopolymers obtained using FLIM was in good agreement with the calculated Flory radius of the respective polymer chain in the coil conformation, allowing predictions about cushion thickness for a given polymer chain length

of lipopolymers. A direct consequence of the polymer-mediated bilayer uplift is the reduction of bilayer-substrate interactions, leading to enhanced bilayer fluctuations. For example, previously reported combined neutron reflectometry and fluorescence microscopy experiments showed that an increase of a polyelectrolyte cushion thickness from 17 to 90 nm is associated with a substantial enhancement of membrane fluctuations [133]. In addition to bilayer-substrate distance, properties of a polymer-cushioned bilayer may also depend on other factors, such as polymer viscoelasticity and bilayer diffusivity. The following two chapters investigate the role of these factors on the properties of physisorbed PTLBs, which have been previously employed as tunable cell surface mimetics.

3.2.2. Obstructed diffusion and interleaflet coupling of obstructed diffusion in a physisorbed PTLB

Incorporation of polymer spacers, with a known concentration, has been shown to allow adjustment of frictional coupling between membrane proteins and the underlying solid substrate [108]. Another key signature of PTLBs is the presence of polymer-tethered lipids or polymer-tethered proteins in the bilayer. They not only play an important role in the stabilization of the PTLB, but also have a profound influence on the lipid diffusion properties of the bilayer. While there is a relatively weak size dependence of protein lateral diffusion in a free lipid bilayer [134], embedded polymer-tethered membrane constituents in the PTLB cause a substantially enhanced size dependence of lipid/protein diffusion properties. This effect can be best demonstrated in PTLBs comprised of phospholipids and lipopolymers, which allow a precise adjustment of polymer-tethered lipid (lipopolymer) concentration. Due to this ability, physisorbed polymer-tethered lipid bilayers comprised of phospholipids and lipopolymers have previously been introduced as an attractive model membrane platform for the quantitative characterization of obstacle-induced obstructed diffusion, a process challenging to characterize in cellular membranes (Fig. 7a). To study diffusion of membrane constituents, wide-field single molecule fluorescence microscopy experiments were conducted on dye-labeled lipids (TRITC-DHPE) and bacteriorhodopsin (monomeric mutant W80i) in physisorbed PTLBs of varying lipopolymer concentration (Fig. 7b) [112].

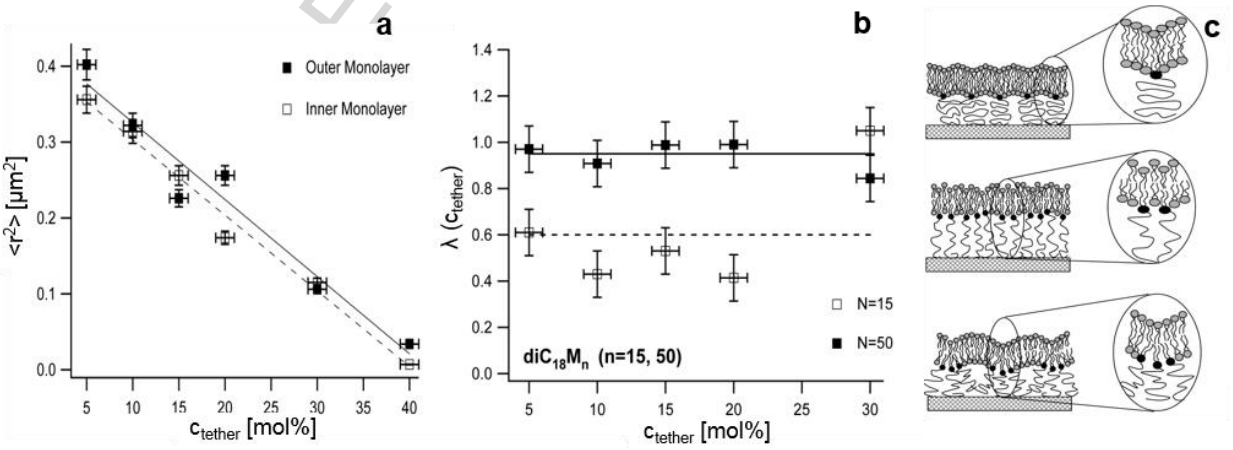

Fig. 7: Leaflet-specific tracking experiments of dye-labeled lipids, shown in (**a**), reveal a strong coupling of obstructed lipid diffusion in a physisorbed PTLB. Lipid tracking data are presented

as mean- square displacement ($<r^2>$) vs tethering concentration (c_{tether}). (**b**) Comparison of inner and outer leaflet lipid tracking data (through coupling parameter λ) demonstrates strong inter-leaflet coupling for longer polymer chain lipopolymers ($diC_{18}M_{50}$) and reduced coupling for shorter polymer chain lipopolymers ($diC_{18}M_{15}$). (**c**) Strong inter-leaflet coupling of obstructed lipid diffusion has been attributed to polymer-induced deformations of the bilayer around tethering points. Reprinted from [130] with permission from publisher.

These single molecule tracking experiments confirmed that, due to the presence of lipopolymers, the lateral diffusion of both TRITC-DHPE, located in the bottom (lipopolymer-containing) leaflet of the bilayer, and the bilayer-spanning W80i mutant are well described by that in a percolating system with distinct percolation thresholds. Moreover, lipid diffusion data were determined to be in good agreement with a free area model of obstructed diffusion, suggesting repulsive interactions between lipid tracers and tethered lipids. Comparison of lipid tracking data with Monte Carlo simulations also showed that lipopolymers in the bottom leaflet of the bilayer behave like immobile obstacles. Furthermore, cumulative distribution function (CDF) analysis indicated Brownian lipid diffusion at low to medium lipopolymer concentration, but anomalous lipid diffusion at elevated tethering densities. (Fig. 7c) These CDF data suggest the random distribution of lipopolymers in the PTLB at lower tethering and the assembly into small lipopolymer aggregates at higher tethering concentration. It should be noted that reported diffusion data may depend on multiple factors, including the chemical nature of the polymer, the viscosity and thickness of the polymer layer, and the type of linkage between polymer chains and solid substrate. For example, there have been reports where no notable obstruction of lipid diffusion over a limited concentration of lipopolymers with reactive groups was observed [135].

Leaflet-specific tracking experiments of TRITC-DHPE revealed that lipopolymers in the bottom leaflet of a physisorbed PTLB also cause obstructed lipid diffusion in the opposite (lipopolymer-free) leaflet of the bilayer, indicating a strong interleaflet coupling of obstructed diffusion [130]. Here TRITC-DHPE tracking experiments in the top leaflet of the bilayer mirrored those obtained in corresponding inner leaflet studies, displaying again Brownian diffusion behavior at low to medium lipopolymer concentrations and anomalous diffusion at elevated lipopolymer content (Fig. 8a). Strong interleaflet coupling of obstructed TRITC-DHPE diffusion was observed regardless of variations in polymer moiety [poly(ethylene glycol), poly(2-methyl-2-oxazoline), and poly(2-ethyl-2-oxazoline)] of lipopolymers. Systematic analysis of lipid tracking data in terms of the parameter λ, which simply describes the ratio of mean-square-displacement values of TRITC-DHPE from tracking experiments in the inner vs outer monolayers, provided valuable insight into the strength of coupling of obstructed lipid diffusion (Fig. 8b). This analysis demonstrated that the coupling of obstructed lipid diffusion depends on the molecular weight of the polymer moiety of lipopolymers, but remains largely unchanged by a variation of lipopolymer concentration, c_{tether}, at least, within a range of $0 \leq c_{tether} \leq 20$ mol%. For example, a strong interleaflet coupling of obstructed lipid diffusion was observed for the longer chain poly(2-ethyl-2oxazoline) [DODA-E_n (n=85)] and poly(2-methyl-2-oxazoline) [diC_{18}-M_n (n = 50)] lipopolymers. In contrast, reduced coupling of obstructed diffusion, comparable to that found in a SLB, was observed with shorter chain versions of both types of lipopolymers [DODA-E_n (n = 35) and diC_{18}-M_n (n = 15)]. In light of existing theoretical work on the problem of bent membranes around pinning sites [136-140], the observed interleaflet coupling of obstructed lipid diffusion was attributed to polymer-induced bilayer deformations around membrane pinning sites (Fig. 8c). Indeed, such a scenario is supported through results from control tracking experiments

on physisorbed polymer-tethered lipid bilayers containing phospholipids and cholesterol, which demonstrated that increased bilayer bending stiffness, through addition of cholesterol, leads to reduced interleaflet coupling of obstructed TRITC-DHPE diffusion [112]. Distinct bilayer morphologies presumably also explain the observed differences in obstructed diffusion and coupling of obstructed diffusion of lipids between physisorbed and chemisorbed polymer-tethered lipid bilayers [112, 130, 135]. Interestingly, strong interleaflet coupling of obstructed lipid diffusion was also determined after polymer adsorption to the top leaflet of a SLB [141]. In this case, the diffusion data were explained using a model of slaved diffusion, where a membrane bound polymer moiety, lipids underneath this moiety and the lipids in the bottom leaflet show the same diffusion [142].

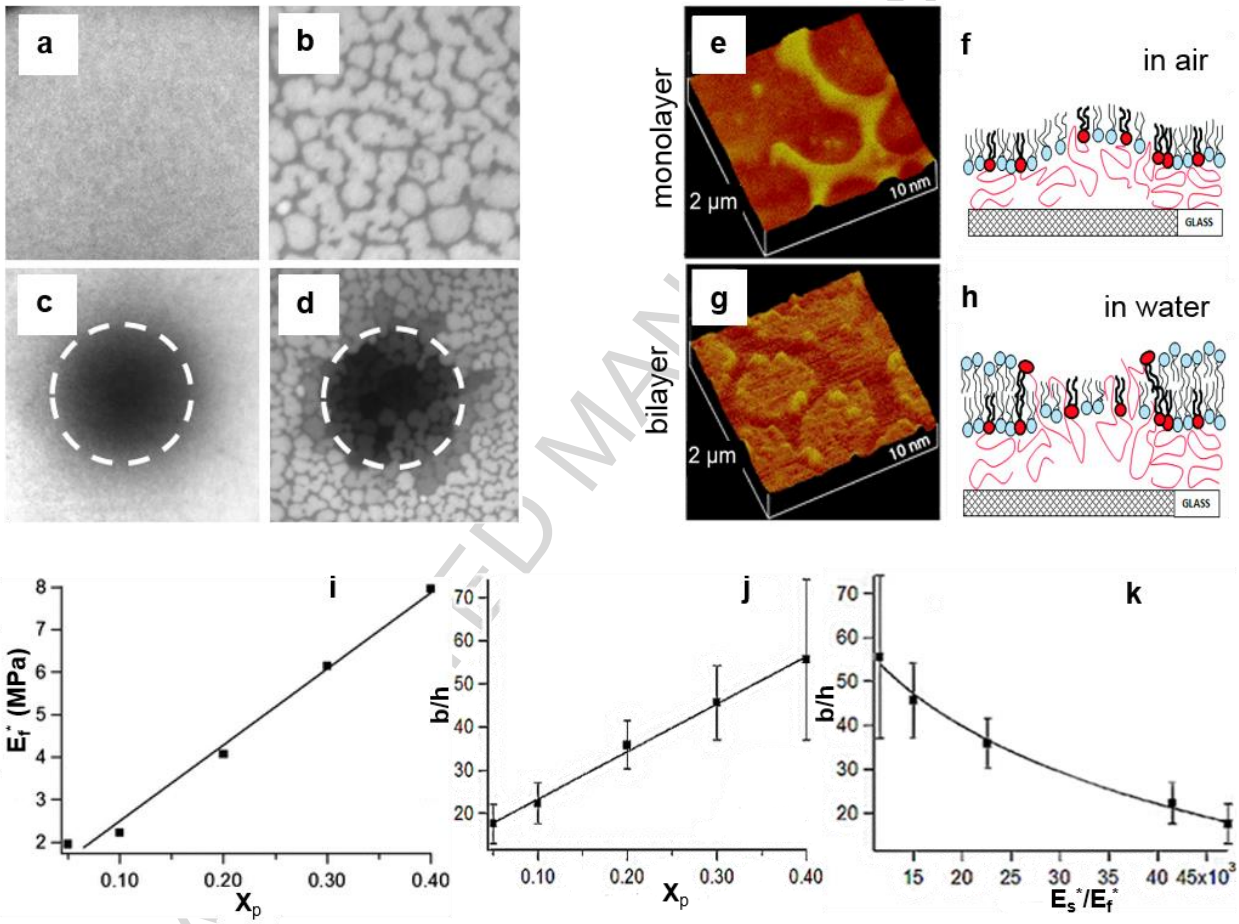

Fig. 8: Lateral stress imposed by elevated concentrations of lipopolymers causes membrane buckling in physisorbed polymer-tethered monolayer and bilayer systems. (**a-b**) Impact of increasing lipopolymer concentrations on fluorescence micrographs of dye-labeled lipids in physisorbed PTLBs. Corresponding spot bleaching experiments reveal that dark areas act as lipid diffusion barriers (**c-d**). Atomic force microscopy data confirm formation of buckling structures in polymer-tethered lipid monolayer (**e**) and compartmentalization of polymer- tethered lipid bilayer (**g**). Model of lipopolymer-induced monolayer buckling (**f**) and compartmentalization of physisorbed polymer-tethered lipid bilayer (**h**), as derived from fluorescence and atomic force microscopy analyses. (**i-k**) Buckling structure information in combination with results from

mean-field theory of polymer-tethered membranes and buckling theory of straight-sided blisters illustrate that variations in lipopolymer concentration lead to changes of elastic properties in a physisorbed polymer-tethered lipid bilayer. (**a-h**) were reprinted from [151] with permission from publisher. (**i-k**) were reprinted from [152] with permission from publisher.

3.2.3. Mechanical properties of PTLB system

One limitation of artificial phospholipid bilayers, as found in liposomes and SLBs, is that they are substantially softer than cellular membranes, making them rather poor biomembrane mimetics in terms of their elastic properties [143, 144]. This limitation can be partially overcome in polymer-supported membrane systems, whose mechanical properties are more similar to those of cellular membranes. Valuable information about mechanical properties of polymer-supported membranes was obtained using the surface forces apparatus (SFA) [145]. These experiments revealed that the presence of the polymer cushion in the membrane system leads to the presence of long-range interaction forces. Moreover, the SFA data showed that the cushion elasticity can be modeled using a simple spring model [145].

Another important aspect represents the tunability of mechanical properties in polymer-supported membranes. For example, lipopolymers in a PTLB not only provide membrane stabilization and enable adjustment of obstructed lipid/protein diffusion, but also allow controlled modification of membrane elasticity. Mean-field calculations previously showed that bilayer bending modulus and compressibility in such membrane systems can be regulated by both the density of polymer-tethered lipids and the molecular weight of tethered polymer chains [146, 147]. Exemplarily, the bending modulus of a red blood cell of 50 k_BT was found to be comparable to that of a polymer-tethered lipid bilayer containing 5 mol% of the poly(ethylene oxide) lipopolymer DSPE-PEG5000, whereas a corresponding membrane system with 20 mol% DSPE-PEG5000 resulted in a bending modulus of 400 k_BT, comparable to that of *Dictyostelium discoideum* (wild type) [148, 149]. The ability to modify membrane elastic properties in liposomes by incorporation of lipopolymers was confirmed experimentally using the micropipette technique [150].

Interestingly, it was also demonstrated that elevated concentrations of lipopolymers lead to membrane buckling, a stress relaxation phenomenon, in physisorbed polymer-tethered monolayer and bilayer systems without exhibiting phospholipid-lipopolymer phase separation (Fig. 9) [151]. Formation of a homogeneous bilayer was reported on top of a buckled polymer-tethered lipid monolayer containing poly(2-methyl-2-oxazoline) lipopolymers. However, bilayer formation on top of buckled monolayer regions was precluded in the presence of the less hydrophilic poly(2-ethyl-2-oxazoline) and poly(ethylene oxide) lipopolymers, leading to the compartmentalization of the polymer-tethered membrane into 1-2 μm compartments at higher lipopolymer concentrations. FRAP using dye-labeled lipids and long-term tracking experiments using quantum dot-conjugated lipids confirmed that buckling-induced compartment boundaries act as diffusion barriers, causing length scale-dependent diffusion properties, with remarkable parallels to those found in plasma membranes. Buckling amplitude and width were previously analyzed as a function of lipopolymer concentration using EPI and atomic force microscopy (AFM). These data could be used to combine mean-field theory of a polymer-tethered membrane with buckling theory of an Euler column to derive a metric between experimentally determined buckling parameters and mechanical membrane properties (Fig. 9 i-k) [152].

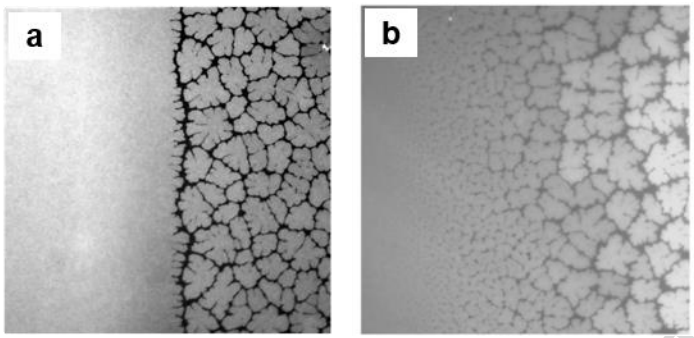

Fig. 9: Controlled adjustment of the lateral distribution of lipopolymers enables fabrication of patterned PTLB systems. Such adjustments may lead to the formation of a sharp boundary between regions of low (no buckling structures) and high (with buckling structures) lipopolymer concentrations (**a**). Alternatively, PTLBs with a lateral gradient in tethering concentration can be achieved (**b**). Results reprinted from [125] with permission from publisher.

3.2.4. Diffusion and elastic properties of polymer-tethered lipid multi-bilayers

Like single PTLBs, polymer-tethered lipid multi-bilayers also allow the controlled adjustment bilayer fluidity. However, the GUV assembly of the latter membrane system, which limits the range of accessible lipopolymer molar concentrations [146], makes modification of bilayer fluidity by variation of lipopolymer concentration impractical. Instead, the lipid lateral diffusion in a polymer-tethered lipid multi-bilayer system of ~50-200 Å thickness can be adjusted by the number of bilayers in the stack. Indeed, systematic lipid tracking experiments in a single polymer-tethered lipid bilayer and the top bilayer of corresponding double, triple, and quadruple bilayer stacks using wide-field single molecule fluorescence microscopy (SMFM) demonstrated a gradual increase of lipid diffusion with increasing degree of bilayer stacking (Fig. 10a). Because the concentration of 5 mol% tethered lipids in these multi-bilayer stacks was previously shown to have no significant influence on obstruction of lipid diffusion [112, 130], the observed diffusion changes could largely be attributed to changes in substrate-bilayer distance, characterized by distinct degrees of frictional coupling between bilayer and underlying solid [153].

Due to the presence of polymer-tethered lipids, polymer-tethered lipid multi-bilayers are also characterized by size-dependent diffusion properties. This feature was previously demonstrated on a polymer-tethered multi-bilayer system, which contained lipid-anchored N-cadherin constructs in its top bilayer [154]. In this case, confocal fluorescence correlation spectroscopy (FCS) experiments showed good lateral mobility of individual N-cadherin constructs in the top bilayer of polymer-tethered multi-bilayer stacks. In contrast, clusters of N-cadherin constructs, induced through adsorption of N-cadherin-functionalized fluorescent beads of 500 nm size, were found to be completely immobilized in the same membrane system. In contrast, similar changes in probe size have substantially less influence on probe diffusivity in a viscous SLB without polymer-tethered lipids [155]. Consistent with the observation of immobilized N-cadherin-coated beads on a polymer-tethered lipid bilayer system with N-cadherin linkers, a predominantly elastic materials response was previously reported in magnetic tweezer microrheometer experiments of laminin-coated superparamagnetic beads, which are bound to the surface of polymer-tethered single and multi-bilayer systems via laminin-laminin linkages (Fig. 10b) [156].

One important outcome from these magnetic tweezer experiments was that elastic compliance does change with an increasing degree of stacking, illustrating the potential suitability of such membrane systems for the analysis of cellular mechanosensitivity. Interestingly, these experiments also showed that the crosslinked laminin coating on the multi-bilayer surface partly contributes to the overall bead response. The latter finding suggests that cellular tractions on laminin-coated polymer-tethered multi-bilayer systems should, at least in part, be attributed to the presence of the crosslinked laminin layer on the surface of the cell surface mimetic.

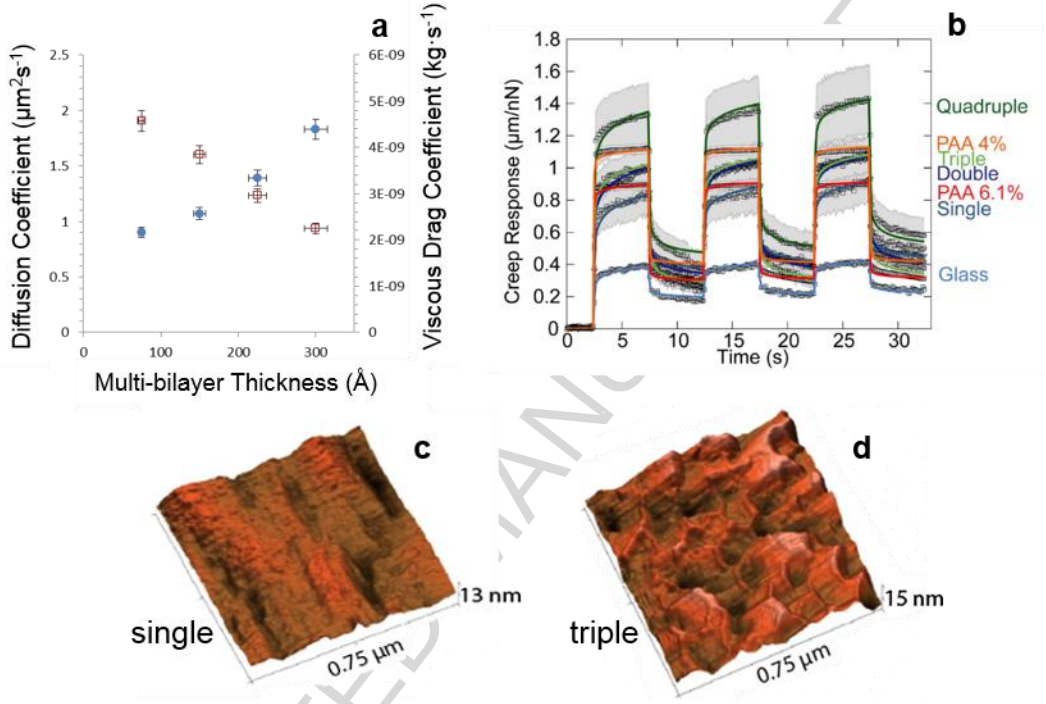

Fig. 10: Single molecule tracking analysis, (**a**), shows gradually increasing diffusion of dye-labeled lipids with increasing bilayer-substrate distance in the multi-bilayer stack. Magnetic tweezer analysis, shown in (**b**), of bilayer-attached magnetic beads reveals that increasing bilayer number decreases film elasticity in the multi-bilayer system. Atomic force microscopy shows that increasing bilayer stacking from single (**c**) to triple (**d**) leads to less planar surface morphology. Results shown in (**a**, **c**-**d**) were reprinted from [118] and **b** was reprinted from [156] with permission from the publishers.

3.3. Cell spreading and migration on PTLB substrates

The size-dependent diffusion properties in lipopolymer-containing PTLBs, discussed in Section 3.2.1, suggest the potential suitability of these model membranes as artificial cell surface-mimicking substrates for the analysis of cell spreading and migration. In this case, the PTLB contains a well-defined amount of reactive lipids, which serve as anchor sites for ligands. Adjustment of ligand density can be accomplished by controlling the molar concentration of reactive lipids in the bilayer of the cell surface mimetic. Previously it was reported that 3T3 fibroblasts, which are known for their ability to develop substantial pulling forces, readily adhere and spread on a physisorbed PTLB that is surface-functionalized with laminin ligands (attached

to thiol lipids in the bilayer using a maleimide-NHS ester crosslinker molecule) [156, 157]. Minner et al. conducted several complementary experiments, which confirmed the integrity of the PTLB substrate in the presence of plated cells [157]. In one set of experiments, confocal spot bleaching of dye-labeled lipids in a laminin-coated PTLB underneath FA regions of plated 3T3 fibroblasts confirmed good fluorescence recovery, which was comparable to corresponding fluorescence recovery results obtained from cell-free PTLB regions (Fig. 11 a-d). In another set of experiments, the cellular phenotype of 3T3 fibroblasts was compared 20 and 40 h after plating. These experiments determined a small, unchanged population of stress fiber-laden polygonic cells of less than 4%, a substantial reduction of crescent cell shapes from 44% (20h) to 14% (40h), and an increase of spindle-like cells from 18% (20h) to 38 at (40h), as well as an increase of dendritic phenotypes from 5% (20h) to 18% (40h). More importantly, no increase of stress fiber-forming cells was observed over time, confirming the inability of plated cells to directly bind to the glass substrate by penetrating through potential bilayer defects.

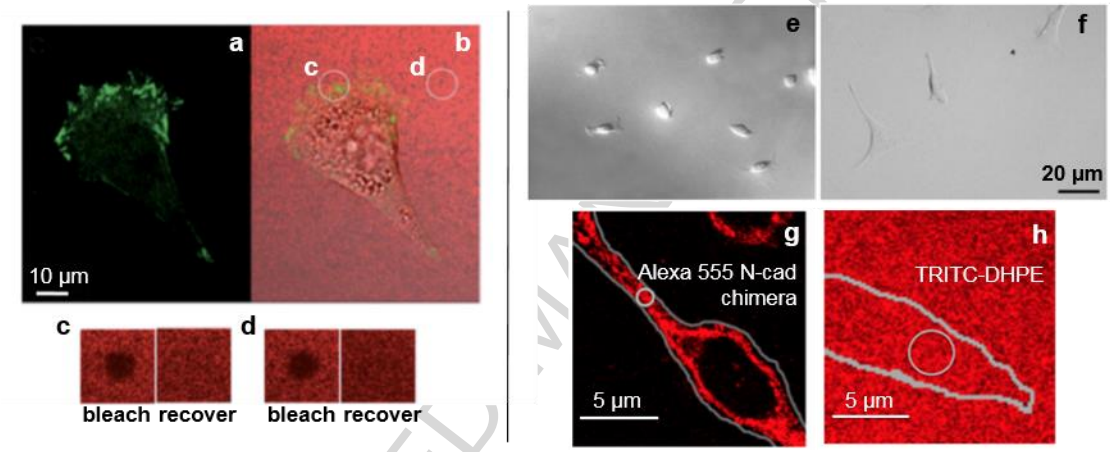

Fig. 11: In this confocal experiment, FA regions were visualized using GFP-FAK (**a**), a marker of cellular FAs, and the integrity of the PTLB system was monitored using the dye-labeled lipid TR-DHPE, (**b**). Individual FRAP experiments were conducted underneath FA regions in (**c**) and outside cells in (**d**)**;** each area shows fluorescent lipid recovery after bleaching. C2C12 myoblasts are unable to spread on a linker-free PTLB (**e**), but display good spreading on a PTLB with N-cadherin linkers (**f**). Plated C2C12 myoblasts cause the accumulation of N-cadherin linkers in a PTLB (**g**), but have no influence on the homogeneous distribution of dye-labeled lipids (**h**) in such a planar membrane. Images in (**a-d**) were reprinted from [157], (**e-h**) were reprinted from [154] with permission from publishers.

While the above described experiments with 3T3 fibroblasts on laminin-coated PTLB systems confirmed the general suitability of PTLBs as engineered cell substrates, the ultimate potential of PTLBs as advanced cell surface mimetics was demonstrated more recently using C2C12 myoblasts on PTLB surfaces with embedded N-cadherin chimera [154]. In this sample architecture, individual His-tagged N-cadherin ectodomain constructs are directly conjugated to lipids with a Ni-chelator group in the PTLB. Unlike laminin ligands, which are able to crosslink [158], lipid-anchored N-cadherin chimera are free to diffuse in the PTLB, as verified by FCS autocorrelation analysis and PCH method. In contrast, clusters of lipid-anchored N-cadherin chimera, induced by binding of N-cadherin-functionalized fluorescent beads (size: 500 nm), were immobilized in the same membrane system, illustrating the size-dependent diffusion

properties of PTLBs. Importantly, analysis of plated cells established that C2C12 myoblasts are able to adhere and spread on a PTLB with N-cadherin ligands, whereas cell spreading was efficiently suppressed on a corresponding ligand-free substrate (Fig. 11e) [154]. Confocal experiments demonstrated furthermore that dye-labeled N-cadherin chimera accumulate into larger cluster assemblies underneath C2C12 cells (Fig. 11g). These clusters are heterogeneously distributed, thereby exhibiting enrichment at the periphery and extensions of adhering cells. Accompanying FRAP experiments determined a partial fluorescence recovery of N-cadherin chimera within such clusters of about 40%, in good agreement with similar results of cadherin diffusion in cellular adherens junctions [154]. While accumulation of mobile ligands into clusters at adhesion sites is a common feature during cell/vesicle adhesion on SLBs and PTLBs, which are both characterized by comparable lipid lateral mobility, the latter membrane system is distinct in its ability to enable accumulation of linkers into linker clusters without impairing cell spreading and migration. This peculiar behavior can be attributed to the size-dependent diffusion properties in PTLBs, enabling lateral diffusion of single lipids and other lipid-anchored molecules, but suppressing the mobility of corresponding molecular clusters.

Another potentially attractive feature of PTLBs as a cell surface-mimicking cell substrate was previously demonstrated by conducting a spatiotemporal analysis of dye-labeled N-cadherin chimera in the presence of plated C2C12 cells. These experiments revealed the long-range movement of N-cadherin clusters underneath migrating cells (Fig. 12a-e), thereby displaying remarkable parallels to corresponding movements of cellular contacts between polarized cells [44, 45, 154]. Because lipid-anchored N-cadherin clusters are unable to freely diffuse in a PTLB, their long-range movement underneath adhering cells should be attributed to cytoskeleton-induced cellular pulling forces. Consistent with this interpretation, formation and long-range movement of N-cadherin clusters was largely suppressed after addition of blebbistatin, a myosin II inhibitor, illustrating the importance of the cytoskeleton of adhering cells in the observed cluster movement of N-cadherin chimera on the PTLB surface Fig. 12f, g. Here cluster tracking analysis revealed the blebbistatin-induced slowdown and eventual dissolution of Alexa 555 labeled N-cadherin chimera clusters on the PTLB surface.

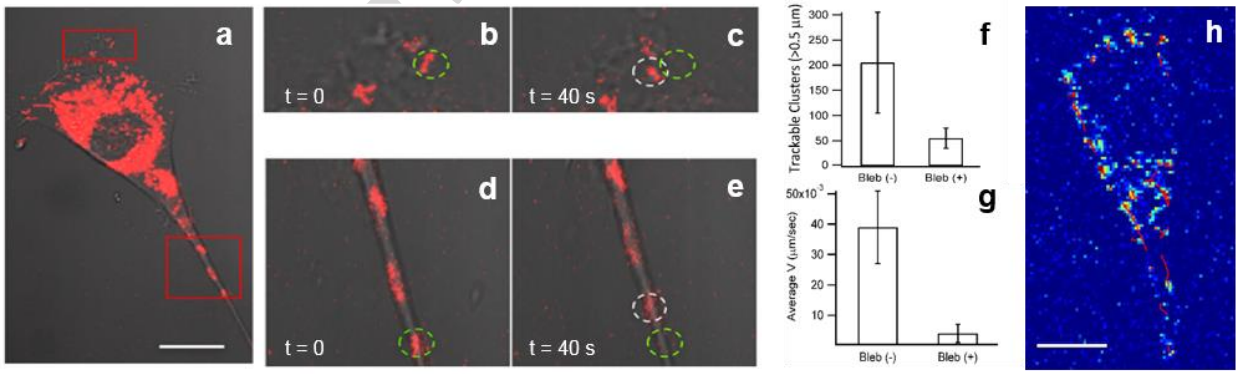

Fig. 12: Spatiotemporal analysis of a PTLB functionalized with Alexa 555-labeled N-cadherin chimera illustrates accumulation of N-cadherin linkers into linker clusters (**a**). Cluster analysis reveals long-range movements of clusters underneath migrating cell (**b-e**). Blebbistatin treatment shows reduction of cluster size (**f**) and mobility (**g**). Cell depicted in (**h**), shows the tracking program used to analyze confocal imaging data, revealing cluster size, speed, and number from time lapse imaging. Figure was reprinted from [154] with permission from publisher.

Taken together, the described experiments of C2C12 myoblasts on N-cadherin-functionalized PTLBs demonstrate that this artificial cell substrate fulfills several important requirements for a cell surface mimetic, which include: (i) the free assembly of ligands into ligand clusters underneath cellular contacts and (ii) the ability of adhering cells to develop cellular tractions, enabling cell spreading and migration. Moreover, these substrates better replicate the long-range movements of adhesion clusters at cell-cell contacts than traditional polymeric films with chemically conjugated linkers. It should be mentioned that the application of PTLBs has not been limited to the characterization of 3T3 fibroblasts and C2C12 myoblasts. In another study, a similar membrane architecture was successfully employed to monitor different stages of neuronal network formation using a PTLB system [159].

3.4. Adjusting substrate mechanical properties in PTLBs to analyze cellular mechanosensitivity

3.4.1. Single PTLB of varying lipopolymer concentrations

Previous advancements in the understanding of cellular mechanosensitivity have been closely linked to the development of engineered cell substrates which allow the controlled adjustment of substrate stiffness. Similarly, substrate mechanical properties in a single PTLB can be altered by changing the concentration of polymer-tethered lipids in the bilayer (discussed in Chapter 3.2.2). Tunable material properties illustrate the potential of PTLBs to serve as cell surface-mimicking materials for the analysis of cellular mechanosensitivity. The impact of such lipopolymer adjustments on properties of plated cell is shown in Fig. 13. Specifically, the micrograph in the upper left of Fig. 13 illustrates the spreading of GFP-actin transfected 3T3 fibroblasts on a single, laminin-coated PTLB substrate, which is characterized by a sharp boundary (yellow dashed line) between regions of high (left side) and low lipopolymer concentrations (right side). It demonstrates that elevated lipopolymer concentrations lead to: (i) increased cell spreading areas and (ii) more pronounced actin stress fibers. As depicted in the histogram in the bottom left of Fig. 13, increased cell spreading can also be observed on homogeneous PTLBs of gradually increasing lipopolymer concentrations. The observed cell behavior in Fig. 13 correlates well with the known impact of lipopolymer concentration on film elasticity in a single PTLB (discussed in 3.1.3). The micrograph in the upper left of Fig. 13 also illustrates the ability to combine single PTLBs with membrane patterning strategies, including those that were described in Section 3.1.3.

3.4.2. Polymer-tethered lipid multi-bilayers

Polymer-tethered multi-bilayers can also be applied as cell substrates for cellular mechanosensing studies. As described in Section 3.2.3, the diffusion and mechanical properties in such multi-bilayer systems can be modified by altering the number of bilayers in the polymer-tethered multi-bilayer stack. While diffusion experiments confirmed increases in lipid diffusivity with increasing stacking [157], corresponding bead rheology measurements established that such adjustments of bilayer number reduce the stiffness of the multi-bilayer substrate [156]. The observed tunable properties have been attributed to the intricate coupling phenomena in polymer-tethered multi-bilayer systems, which include strong interleaflet coupling of immobilized

membrane constituents, coupling of obstructed diffusion, and coupling by lipopolymer-mediated inter-bilayer connections [120, 130, 142].

To test the suitability of polymer-tethered lipid multi-bilayers for the analysis of cellular mechanosensitivity, properties of 3T3 fibroblasts were previously analyzed on such membrane systems containing laminin ligands [156]. In these experiments, cell spreading area was found to

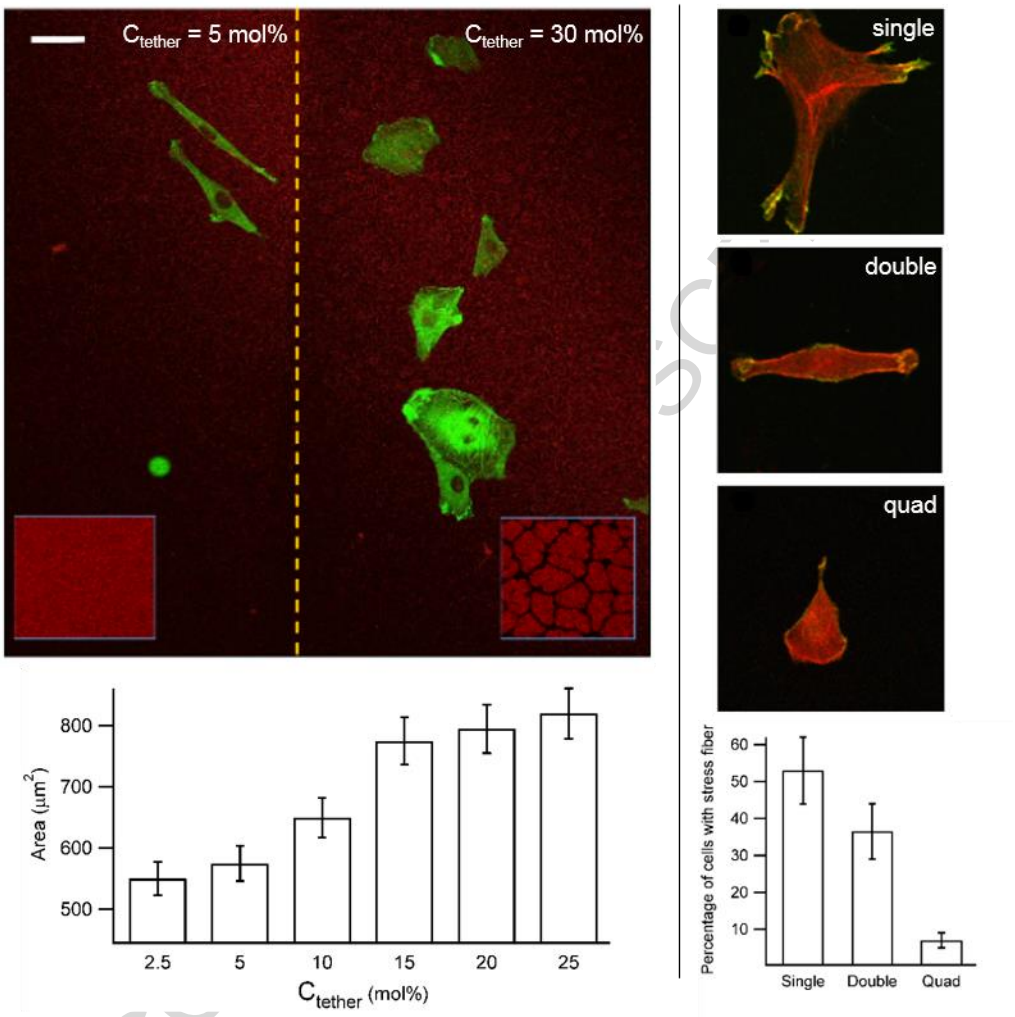

Fig. 13: Cell spreading area depends on concentration of lipopolymers in a single PTLB, as illustrated on a patterned PTLB with sharp boundary (micrograph in upper left), illustrated by the yellow dashed line, between regions of high (right side) and low (left side) tethering concentrations (insets illustrate differences in membrane buckling). Gradual increase of lipopolymer concentration (c_{tether}) causes an increase in cell spreading area in single PTLB, histogram shown in bottom left. Immunofluorescence micrographs show substantial differences in cell spreading, actin organization (red channel), and β-catenin (green channel) distribution on N-cadherin-functionalized PTLB systems with one to four bilayers in a stack. These changes in bilayer stacking have a profound impact on the population of stress fiber-forming cells (histogram shown in bottom right). Data shown on the right were reprinted from [154] with permission from publisher.

show a statistically significant ($p < 0.05$) inverse correlation with the elastic compliance of the substrate, meaning that cell area decreases with increasing number of bilayer stacks. Interestingly, changes in bilayer stacking between single and quadruple bilayer systems had a similar impact on cell spreading area, as variations in substrate stiffness between 4% and 6.1% PAA gels.

Several groups have previously reported phenotype transitions in 3T3 fibroblasts in response to substrate elasticity and in all cases cells have displayed rounder shapes, and at times an increased tendency to form cellular extensions when plated on softer hydrogel substrates [33, 35, 160]. Similarly, experiments on laminin-functionalized polymer-tethered single and multi-bilayer systems have demonstrated that 3T3 cells alter their phenotype as a function of bilayer stacking [157]. These experiments also determined that changes in bilayer stacking affected cytoskeleton organization as well. On laminin-coated glass, EPI micrographs of 3T3 fibroblasts predominantly showed polygonic and crescent shapes, a typical cellular response to a rigid substrate. On single bilayer substrates, the overall number of cells with static stress fibers was greatly reduced and cortical actin structures emerge; however, the overall cellular phenotype distribution is similar to the phenotypes on glass. On double bilayer substrates, these stress fiber-laden shapes are almost completely replaced with polarized phenotypes exhibiting lamellipodium-like regions at one end and stretched processes at the opposite end. Here, cells take on more spindle-like shapes and show an enhanced ability to form dendritic-like extensions, and typically display a meshwork of cortical actin structures evenly distributed throughout the cell with short, radially-oriented actin bundles at the leading edge. On quadruple bilayers, spindle-like shapes become most prevalent and their stretched processes span distances of up to 50 μm. The fraction of cells showing these processes increases with bilayer stacking: on single bilayers only 22% of the cells show extensions of more than 5 μm but this value increases to approximately 39% and 57% on double and quadruple bilayer systems, respectively [157]. Moreover, comparison of these results with microrheology data of cell-bound superparamagnetic beads show that the stiffness of cells plated on polymer-tethered lipid multi-bilayers decreases with increasing number of bilayers in the multi-bilayer stack [see Fig. 14e]. These results demonstrate a direct correlation between substrate stiffness and the extent of cellular stress fiber formation [156].

More recently, the functionality of polymer-tethered multi-bilayers for the characterization of cellular mechanosensitivity has also been tested on C2C12 myoblasts, which are bound to the biomembrane-mimicking substrate via N-cadherin linkages [154]. In good agreement with results obtained on laminin-coated PTLB systems, changes in bilayer stacking have a notable impact on both cell morphology and cytoskeletal organization (Fig. 13). Myoblasts on single bilayer architectures frequently display polygonic morphologies with well-developed ventral stress fibers spanning the entire cell, whereas those on multi-bilayer substrates lack visible actin stress fibers and show less pronounced AJ formation. Furthermore, analysis of β-catenin, an AJ marker, demonstrates that changes in bilayer stacking influence AJ formation. Consistent with these findings, the population of stress fiber-forming cells decreases with increasing numbers of bilayer in the stack.

3.4.3. Polymer gel-tethered lipid bilayer and traction force microscopy

Cellular traction forces are generated through mechanotransduction pathways and are transduced through the cell by the cytoskeleton to cell adhesion sites, such as FAs and AJs. Previously,

traction force microscopy was introduced to probe cellular contractility on surface-functionalized PAA gels of known stiffness. Here embedded fluorescent beads were employed to monitor deformations of the gel by cellular contractile forces. Since cell tractions are counter-balanced by equal and opposite substrate forces, the displacement of marker beads at the surface of the PA gel allows computation of cell tractions. To test the functionality of polymer-tethered multi-bilayers for the analysis of cellular mechanosensitivity, Lautscham et al. previously introduced a modified traction force microscopy assay that enables analysis of cellular tractions on PTLB substrates (Fig. 14 a-d) [156].

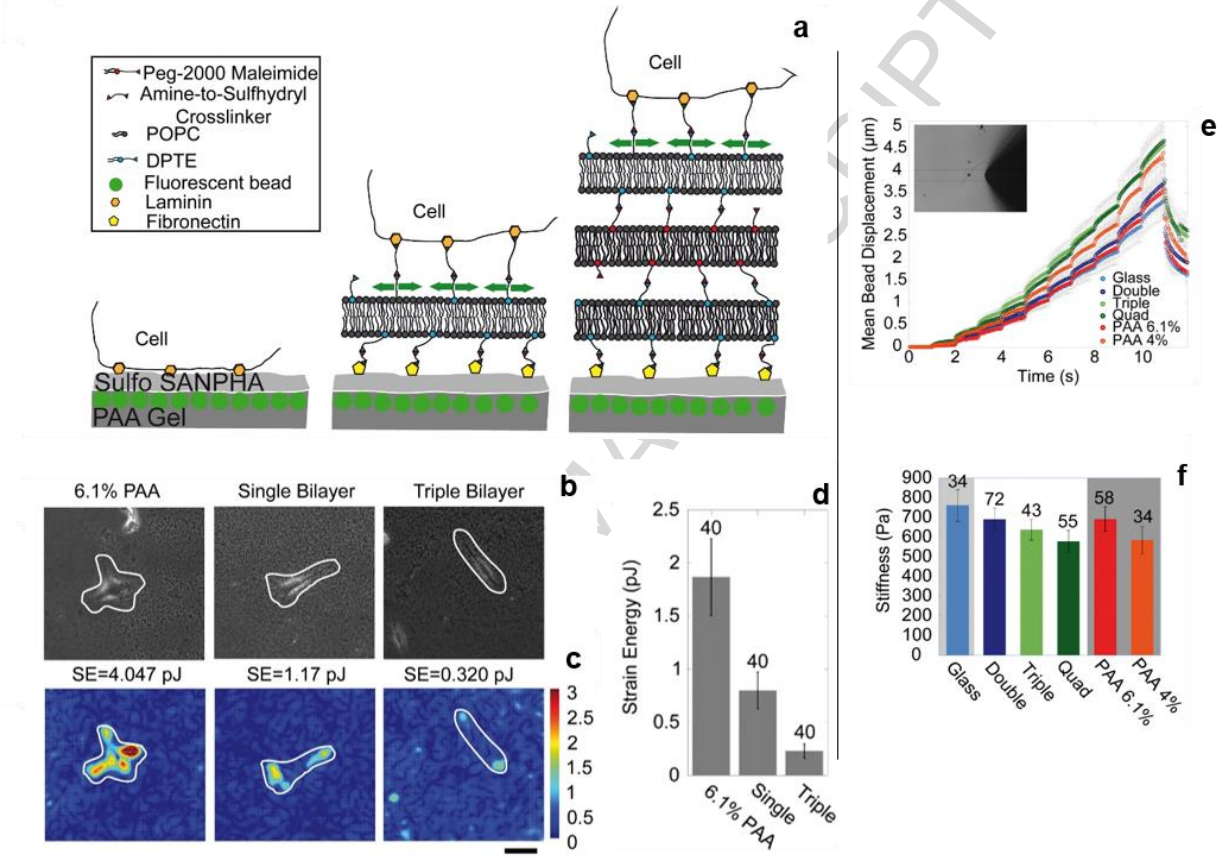

Fig. 14: Schematic of traction force microscopy assay in the presence of PTLB systems (**a**), showing the coupling architecture between functionalized lipid bilayer and polymer gel. Representative results from such an assay show that cells sense the decrease in elasticity with increased bilayer stacking, results include cellular contact areas (**b**), related traction force data (**c**), and resulting strain energies (**d**). Data showing the displacement of magnetic beads attached to cells on different types of substrates (**e-f**), which include glass, PTLB with one and three bilayers, and two different types of PAA gels (4 and 6.1%). These bead rheology data illustrate that the stiffness of plated MEF cells decreases with increasing bilayer number in a multi-bilayer stack. Figure was reprinted from [156] with permission from publisher.

In this assay, a laminin-functionalized PTLB was chemically coupled to a PAA gel of known stiffness with embedded fluorescent beads. Plated cells were found to readily spread on such a polymer gel-tethered lipid bilayer system. The largest contractile forces were observed for cells

plated directly on the laminin-functionalized hydrogel and the strain energy was seen to decrease on both single and even more so on triple bilayer substrates. This decrease in traction forces on softer more dissipative bilayer stacks can be attributed to a decreased cytoskeletal-based contractile prestress, which corresponds well with cell behavior on elastic PAA substrates [32, 36, 161, 162]. Analysis of traction force data also suggest that not only the mechanical properties of the polymer-tethered multi-bilayer itself, but also those of the potentially crosslinked laminin coating may contribute to the overall cell response. A comparable traction force assay was recently introduced to probe cellular contractile forces of C2C12 myoblasts on PTLB systems with N-cadherin linkers, which are unable to crosslink [154]. Again these experiments identified reduced cell-generated traction forces with increasing number of bilayers in the stack, in good agreement with the observed data of cytoskeletal organization, which exhibit reduced stress fiber formation with stacking in a corresponding artificial cell substrate.

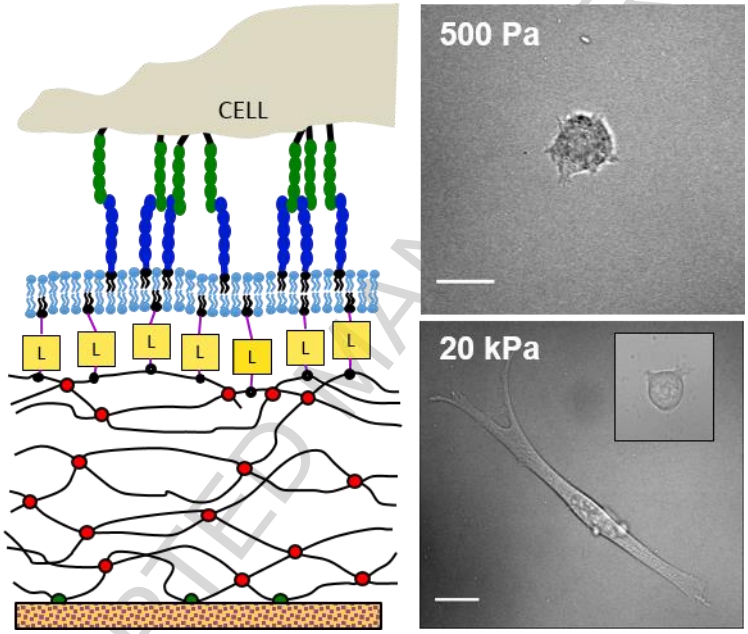

Fig. 15: Schematic on the left shows the architecture of a polymer gel-tethered lipid bilayer. C2C12 myoblasts plated on a N-cadherin-functionalized polymer gel-tethered lipid bilayer show a round morphology on a soft (500 Pa) PAA film, but display stretched morphologies on corresponding substrates with a more rigid (20 kPa) PAA layer (inset presents control on 20 kPa substrate without N-cadherin linkers). Scale bars: 20µm.

Importantly, polymer gel-tethered lipid bilayers are useful for more than the described traction force microscopy assay. If correctly designed, they represent a very advanced PTLB, which can stand on its own as a cell surface-mimicking cell substrate. In fact, substrate mechanical properties in such a membrane architecture can simply be altered over a wide range of elasticities by adjusting crosslinking density of the underlying polymeric gel. The impact of such substrate stiffness modifications on cell spreading is illustrated in Fig. 15. While plated C2C12 myoblasts display a round morphology on a N-cadherin-functionalized polymer-gel tethered lipid bilayer with a PAA film of 500 Pa (Fig. 15, upper right), they show predominantly stretched morphologies on a corresponding substrate with a PAA film of 20 kPa (Fig. 15 lower right). It should be emphasized that a comparably large range of elasticity adjustments cannot be

achieved with other PTLB designs discussed above. Interestingly, an alternative approach of substrate tunability in a polymer-supported lipid bilayer system was recently demonstrated using a different type of film design, in which a thin polymer layer was introduced as lubricant film between underlying polymer gel and phospholipid bilayer [163].

4. Conclusion and Outlook

As reported previously, the functionalization of polymeric materials of controlled stiffness with ligands for cell adhesion receptors improved our understanding about important mechanisms of cell migration and cellular mechanosensitivity in an ECM environment. The current review on cell surface mimetics illustrates that an alternative biomimetics strategy involving fluid lipid bilayers can be applied to decipher the underlying molecular processes during similar cellular processes across the cell-cell interface, which are currently less well understood [15, 164]. Cellular processes across the cell-cell interface are considered to be significant in processes such as embryonic development and wound healing. In particular, the PTLB architecture represents a promising artificial cell substrate strategy for the characterization of cellular mechanosensing because it allows the controlled adjustment of substrate mechanical properties without hindering the free assembly of ligands on the substrate surface. These capabilities open the door for the characterization of molecular processes during the force/substrate stiffness-regulated formation and maturation of cellular adhesions. An intriguing expansion of current cell surface mimetic concepts will be the inclusion of molecular assembly strategies utilized for the design of synthetic cells, in which crosslinked actin filaments are attached to adhesion proteins via more realistic protein linkages [165, 166]. Such advanced assembly concepts could be particularly beneficial in improving our understanding about the interplay between cellular signaling and the regulation of cell adhesion protein assembly and disassembly during cell processes, such as cell migration. Another potentially fascinating expansion could be the characterization of cellular properties in microchannels, which are surface-functionalized with cell surface mimetics, thus creating a quasi-3D environment for migrating cells. A first step into this direction has been the design of a SLB-coated microchannel as a biomembrane-mimicking cell substrate [167]. In this case, a PDMS microwell platform was surface-coated with a SLB and E-cadherin constructs were specifically linked to the lipid bilayer using biotin-streptavidin coupling to explore the impact of E-cadherin linker mobility on shape and cytoskeletal organization of CHO cells inside the microchannel. Based on current PTLB fabrication methods, it should be technically feasible to build PTLB-coated microchannels, which can be employed in quasi-3D cellular studies.

Acknowledgements
This work was in part supported by the National Science Foundation (grant: DMR 1006552) and the IUPUI Integrated Nanosystems Development Institute.

References

[1] I. Patla, T. Volberg, N. Elad, V. Hirschfeld-Warneken, C. Grashoff, R. Fassler, J.P. Spatz, B. Geiger, O. Medalia, Dissecting the molecular architecture of integrin adhesion sites by cryo-electron tomography, Nat Cell Biol, 12 (2010) 909-915.

[2] P. Kanchanawong, G. Shtengel, A.M. Pasapera, E.B. Ramko, M.W. Davidson, H.F. Hess, C.M. Waterman, Nanoscale architecture of integrin-based cell adhesions, Nature, 468 (2010) 580-584.

[3] H. Wolfenson, I. Lavelin, B. Geiger, Dynamic Regulation of the Structure and Functions of Integrin Adhesions, Dev Cell, 24 (2013) 447-458.

[4] B. Geiger, J.P. Spatz, A.D. Bershadsky, Environmental sensing through focal adhesions, Nat Rev Mol Cell Bio, 10 (2009) 21-33.

[5] H. Wolfenson, Y.I. Henis, B. Geiger, A.D. Bershadsky, The Heel and Toe of the Cell's Foot: A Multifaceted Approach for Understanding the Structure and Dynamics of Focal Adhesions, Cell Motil Cytoskel, 66 (2009) 1017-1029.

[6] B. Wehrle-Haller, Structure and function of focal adhesions, Current Opinion in Cell Biology, 24 (2012) 116-124.

[7] P.W. Oakes, M.L. Gardel, Stressing the limits of focal adhesion mechanosensitivity, Current Opinion in Cell Biology, 30 (2014) 68-73.

[8] D.E. Leckband, Q. le Duc, N. Wang, J. de Rooij, Mechanotransduction at cadherin-mediated adhesions, Curr Opin Cell Biol, 23 (2011) 523-530.

[9] E. Papusheva, C.P. Heisenberg, Spatial organization of adhesion: force-dependent regulation and function in tissue morphogenesis, Embo J, 29 (2010) 2753-2768.

[10] W. Engl, B. Arasi, L.L. Yap, J.P. Thiery, V. Viasnoff, Actin dynamics modulate mechanosensitive immobilization of E-cadherin at adherens junctions, Nature Cell Biology, 16 (2014) 584-+.

[11] J.C. Sandquist, W.M. Bement, Hold on tightly, let go lightly: myosin functions at adherens junctions, Nature Cell Biology, 12 (2010) 633-635.

[12] K. Burridge, M. ChrzanowskaWodnicka, Focal adhesions, contractility, and signaling, Annual Review of Cell and Developmental Biology, 12 (1996) 463-518.

[13] A.D. Bershadsky, N.Q. Balaban, B. Geiger, Adhesion-dependent cell mechanosensitivity, Annual Review of Cell and Developmental Biology, 19 (2003) 677-695.

[14] M. Lambert, O. Thoumine, J. Brevier, D. Choquet, D. Riveline, R.M. Mege, Nucleation and growth of cadherin adhesions, Exp Cell Res, 313 (2007) 4025-4040.
[15] S.M. Troyanovsky, Mechanism of cell-cell adhesion complex assembly, Current Opinion in Cell Biology, 11 (1999) 561-566.
[16] B. Baum, M. Georgiou, Dynamics of adherens junctions in epithelial establishment, maintenance, and remodeling, Journal of Cell Biology, 192 (2011) 907-917.
[17] B. Geiger, A. Bershadsky, R. Pankov, K.M. Yamada, Transmembrane extracellular matrix-cytoskeleton crosstalk, Nat Rev Mol Cell Bio, 2 (2001) 793-805.
[18] S.M. Schoenwaelder, K. Burridge, Bidirectional signaling between the cytoskeleton and integrins, Current Opinion in Cell Biology, 11 (1999) 274-286.
[19] A.L. Berrier, K.M. Yamada, Cell-matrix adhesion, Journal of Cellular Physiology, 213 (2007) 565-573.
[20] B. Geiger, A. Bershadsky, Assembly and mechanosensory function of focal contacts, Current Opinion in Cell Biology, 13 (2001) 584-592.
[21] T.P. Lele, C.K. Thodeti, D.E. Ingber, Force meets chemistry: Analysis of mechanochemical conversion in focal adhesions using fluorescence recovery after photobleaching, J Cell Biochem, 97 (2006) 1175-1183.
[22] C.G. Galbraith, K.M. Yamada, M.P. Sheetz, The relationship between force and focal complex development, Journal of Cell Biology, 159 (2002) 695-705.
[23] D.E. Discher, P. Janmey, Y.L. Wang, Tissue cells feel and respond to the stiffness of their substrate, Science, 310 (2005) 1139-1143.
[24] D.E. Ingber, Cellular mechanotransduction: putting all the pieces together again, Faseb J, 20 (2006) 811-827.
[25] V. Vogel, M. Sheetz, Local force and geometry sensing regulate cell functions, Nat Rev Mol Cell Bio, 7 (2006) 265-275.
[26] F.J. Alenghat, D.E. Ingber, Mechanotransduction: all signals point to cytoskeleton, matrix, and integrins, Sci STKE, 2002 (2002) pe6.
[27] P.A. Janmey, C.A. McCulloch, Cell mechanics: integrating cell responses to mechanical stimuli, Annu Rev Biomed Eng, 9 (2007) 1-34.
[28] D.E. Ingber, Mechanobiology and diseases of mechanotransduction, Ann Med, 35 (2003) 564-577.

[29] M.J. Paszek, N. Zahir, K.R. Johnson, J.N. Lakins, G.I. Rozenberg, A. Gefen, C.A. Reinhart-King, S.S. Margulies, M. Dembo, D. Boettiger, D.A. Hammer, V.M. Weaver, Tensional homeostasis and the malignant phenotype, Cancer Cell, 8 (2005) 241-254.
[30] M.H. Zaman, L.M. Trapani, A. Siemeski, D. MacKellar, H.Y. Gong, R.D. Kamm, A. Wells, D.A. Lauffenburger, P. Matsudaira, Migration of tumor cells in 3D matrices is governed by matrix stiffness along with cell-matrix adhesion and proteolysis, P Natl Acad Sci USA, 103 (2006) 10889-10894.
[31] D.E. Jaalouk, J. Lammerding, Mechanotransduction gone awry, Nat Rev Mol Cell Bio, 10 (2009) 63-73.
[32] R.J. Pelham, Jr., Y. Wang, Cell locomotion and focal adhesions are regulated by substrate flexibility, Proc Natl Acad Sci U S A, 94 (1997) 13661-13665.
[33] P.C. Georges, P.A. Janmey, Cell type-specific response to growth on soft materials, J Appl Physiol (1985), 98 (2005) 1547-1553.
[34] T. Yeung, P.C. Georges, L.A. Flanagan, B. Marg, M. Ortiz, M. Funaki, N. Zahir, W. Ming, V. Weaver, P.A. Janmey, Effects of substrate stiffness on cell morphology, cytoskeletal structure, and adhesion, Cell Motil Cytoskeleton, 60 (2005) 24-34.
[35] K. Ghosh, Z. Pan, E. Guan, S. Ge, Y. Liu, T. Nakamura, X.D. Ren, M. Rafailovich, R.A. Clark, Cell adaptation to a physiologically relevant ECM mimic with different viscoelastic properties, Biomaterials, 28 (2007) 671-679.
[36] C.M. Lo, H.B. Wang, M. Dembo, Y.L. Wang, Cell movement is guided by the rigidity of the substrate, Biophysical Journal, 79 (2000) 144-152.
[37] P. Friedl, E. Sahai, S. Weiss, K.M. Yamada, New dimensions in cell migration, Nat Rev Mol Cell Bio, 13 (2012) 743-747.
[38] A.J. Engler, S. Sen, H.L. Sweeney, D.E. Discher, Matrix elasticity directs stem cell lineage specification, Cell, 126 (2006) 677-689.
[39] F. Rehfeldt, A.E.X. Brown, M. Raab, S.S. Cai, A.L. Zajac, A. Zemel, D.E. Discher, Hyaluronic acid matrices show matrix stiffness in 2D and 3D dictates cytoskeletal order and myosin-II phosphorylation within stem cells, Integr Biol-Uk, 4 (2012) 422-430.
[40] E. Hachet, H. Van Den Berghe, E. Bayma, M.R. Block, R. Auzely-Velty, Design of Biomimetic Cell-Interactive Substrates Using Hyaluronic Acid Hydrogels with Tunable Mechanical Properties, Biomacromolecules, 13 (2012) 1818-1827.

[41] T. Pompe, M. Kaufmann, M. Kasimir, S. Johne, S. Glorius, L. Renner, M. Bobeth, W. Pompe, C. Werner, Friction-Controlled Traction Force in Cell Adhesion, Biophysical Journal, 101 (2011) 1863-1870.
[42] A.P. Kourouklis, R.V. Lerum, H. Bermudez, Cell adhesion mechanisms on laterally mobile polymer films, Biomaterials, 35 (2014) 4827-4834.
[43] D. Stroumpoulis, H. Zhang, L. Rubalcava, J. Gliem, M. Tirrell, Cell adhesion and growth to Peptide-patterned supported lipid membranes, Langmuir, 23 (2007) 3849-3856.
[44] F. Peglion, F. Llense, S. Etienne-Manneville, Adherens junction treadmilling during collective migration, Nat Cell Biol, 16 (2014) 639-651.
[45] Y. Kametani, M. Takeichi, Basal-to-apical cadherin flow at cell junctions, Nat Cell Biol, 9 (2007) 92-98.
[46] R. Glazier, K. Salaita, Supported lipid bilayer platforms to probe cell mechanobiology, Biochim Biophys Acta, 1859 (2017) 1465-1482.
[47] E.T. Castellana, P.S. Cremer, Solid supported lipid bilayers: From biophysical studies to sensor design, Surf. Sci. Rep., 61 (2006) 429-444.
[48] J.T. Groves, M.L. Dustin, Supported planar bilayers in studies on immune cell adhesion and communication, Journal of Immunological Methods, 278 (2003) 19-32.
[49] M. Tanaka, E. Sackmann, Polymer-supported membranes as models of the cell surface, Nature, 437 (2005) 656-663.
[50] J. Andersson, I. Koper, Tethered and Polymer Supported Bilayer Lipid Membranes: Structure and Function, Membranes, 6 (2016).
[51] W. Knoll, K. Bender, R. Forch, C. Frank, H. Gotz, C. Heibel, T. Jenkins, U. Jonas, A. Kibrom, R. Kugler, C. Naumann, R. Naumann, A. Reisinger, J. Ruhe, S. Schiller, E.K. Sinner, Polymer-Tethered Bimolecular Lipid Membranes, Adv Polym Sci, 224 (2010) 87-111.
[52] L.K. Tamm, H.M. McConnell, Supported phospholipid bilayers, Biophys J, 47 (1985) 105-113.
[53] E. Sackmann, Supported membranes: scientific and practical applications, Science, 271 (1996) 43-48.
[54] A.A. Brian, H.M. McConnell, Allogeneic stimulation of cytotoxic T cells by supported planar membranes, Proc Natl Acad Sci U S A, 81 (1984) 6159-6163.

[55] J. Raedler, H. Strey, E. Sackmann, Phenomenology and Kinetics of Lipid Bilayer Spreading on Hydrophilic Surfaces, Langmuir, 11 (1995) 4539-4548.
[56] S.J. Johnson, T.M. Bayerl, D.C. McDermott, G.W. Adam, A.R. Rennie, R.K. Thomas, E. Sackmann, Structure of an adsorbed dimyristoylphosphatidylcholine bilayer measured with specular reflection of neutrons, Biophys J, 59 (1991) 289-294.
[57] S. Krueger, B.W. Koenig, W.J. Orts, N.F. Berk, C.F. Majkrzak, K. Gawrisch, Neutron reflectivity studies of single lipid bilayers supported on planar substrates, Basic Life Sci, 64 (1996) 205-213.
[58] J. Salafsky, J.T. Groves, S.G. Boxer, Architecture and Function of Membrane Proteins in Planar Supported Bilayers: A Study with Photosynthetic Reaction Centers †, Biochemistry, 35 (1996) 14773-14781.
[59] K. Jacobson, Lateral diffusion in membranes, Cell Motil, 3 (1983) 367-373.
[60] E. Sackmann, The seventh Datta Lecture. Membrane bending energy concept of vesicle- and cell-shapes and shape-transitions, FEBS Lett, 346 (1994) 3-16.
[61] G.I. Bell, M. Dembo, P. Bongrand, Cell adhesion. Competition between nonspecific repulsion and specific bonding, Biophys J, 45 (1984) 1051-1064.
[62] A. Kloboucek, A. Behrisch, J. Faix, E. Sackmann, Adhesion-induced receptor segregation and adhesion plaque formation: A model membrane study, Biophysical Journal, 77 (1999) 2311-2328.
[63] S.F. Fenz, A.-S. Smith, R. Merkel, K. Sengupta, Inter-membrane adhesion mediated by mobile linkers: Effect of receptor shortage, Soft Matter, 7 (2011) 952-962.
[64] A. Albersdorfer, T. Feder, E. Sackmann, Adhesion-induced domain formation by interplay of long-range repulsion and short-range attraction force: A model membrane study, Biophysical Journal, 73 (1997) 245-257.
[65] A. Boulbitch, Z. Guttenberg, E. Sackmann, Kinetics of membrane adhesion mediated by ligand-receptor interaction studied with a biomimetic system, Biophys J, 81 (2001) 2743-2751.
[66] L.B. Smilenov, A. Mikhailov, R.J. Pelham, E.E. Marcantonio, G.G. Gundersen, Focal adhesion motility revealed in stationary fibroblasts, Science, 286 (1999) 1172-1174.
[67] A.S. Smith, K. Sengupta, S. Goennenwein, U. Seifert, E. Sackmann, Force-induced growth of adhesion domains is controlled by receptor mobility, P Natl Acad Sci USA, 105 (2008) 6906-6911.

[68] S.F. Fenz, T. Bihr, D. Schmidt, R. Merkel, U. Seifert, K. Sengupta, A.-S. Smith, Membrane fluctuations mediate lateral interaction between cadherin bonds, Nat. Phys., 13 (2017) 906-913.
[69] R. Parthasarathy, J.T. Groves, Protein patterns at lipid bilayer junctions, Proc. Natl. Acad. Sci. U. S. A., 101 (2004) 12798-12803.
[70] M.L. Dustin, M.E. Sanders, S. Shaw, T.A. Springer, Purified lymphocyte function-associated antigen 3 binds to CD2 and mediates T lymphocyte adhesion, J Exp Med, 165 (1987) 677-692.
[71] C. Wulfing, M.D. Sjaastad, M.M. Davis, Visualizing the dynamics of T cell activation: intracellular adhesion molecule 1 migrates rapidly to the T cell/B cell interface and acts to sustain calcium levels, Proc Natl Acad Sci U S A, 95 (1998) 6302-6307.
[72] S.D. Marlin, T.A. Springer, Purified intercellular adhesion molecule-1 (ICAM-1) is a ligand for lymphocyte function-associated antigen 1 (LFA-1), Cell, 51 (1987) 813-819.
[73] M.L. Dustin, T.A. Springer, Lymphocyte function-associated antigen-1 (LFA-1) interaction with intercellular adhesion molecule-1 (ICAM-1) is one of at least three mechanisms for lymphocyte adhesion to cultured endothelial cells, J Cell Biol, 107 (1988) 321-331.
[74] A. Grakoui, S.K. Bromley, C. Sumen, M.M. Davis, A.S. Shaw, P.M. Allen, M.L. Dustin, The immunological synapse: a molecular machine controlling T cell activation, Science, 285 (1999) 221-227.
[75] C.R. Monks, B.A. Freiberg, H. Kupfer, N. Sciaky, A. Kupfer, Three-dimensional segregation of supramolecular activation clusters in T cells, Nature, 395 (1998) 82-86.
[76] T.A. Springer, Adhesion receptors of the immune system, Nature, 346 (1990) 425-434.
[77] S. Pautot, H. Lee, E.Y. Isacoff, J.T. Groves, Neuronal synapse interaction reconstituted between live cells and supported lipid bilayers, Nat Chem Biol, 1 (2005) 283-289.
[78] C.H. Yu, J.B. Law, M. Suryana, H.Y. Low, M.P. Sheetz, Early integrin binding to Arg-Gly-Asp peptide activates actin polymerization and contractile movement that stimulates outward translocation, Proc Natl Acad Sci U S A, 108 (2011) 20585-20590.
[79] C.H. Yu, N.B. Rafiq, A. Krishnasamy, K.L. Hartman, G.E. Jones, A.D. Bershadsky, M.P. Sheetz, Integrin-matrix clusters form podosome-like adhesions in the absence of traction forces, Cell Rep, 5 (2013) 1456-1468.
[80] R. Changede, X. Xu, F. Margadant, M.P. Sheetz, Nascent Integrin Adhesions Form on All Matrix Rigidities after Integrin Activation, Dev Cell, 35 (2015) 614-621.

[81] C.J. Hsu, W.T. Hsieh, A. Waldman, F. Clarke, E.S. Huseby, J.K. Burkhardt, T. Baumgart, Ligand Mobility Modulates Immunological Synapse Formation and T Cell Activation, Plos One, 7 (2012).
[82] J. Tsai, L.C. Kam, Lateral Mobility of E-cadherin Enhances Rac1 Response in Epithelial Cells, Cell Mol Bioeng, 3 (2010) 84-90.
[83] V.P. Ma, Y. Liu, L. Blanchfield, H. Su, B.D. Evavold, K. Salaita, Ratiometric Tension Probes for Mapping Receptor Forces and Clustering at Intermembrane Junctions, Nano Lett, 16 (2016) 4552-4559.
[84] C.R. Nowosad, K.M. Spillane, P. Tolar, Germinal center B cells recognize antigen through a specialized immune synapse architecture, Nat Immunol, 17 (2016) 870-877.
[85] Y. Liu, L. Blanchfield, V.P. Ma, R. Andargachew, K. Galior, Z. Liu, B. Evavold, K. Salaita, DNA-based nanoparticle tension sensors reveal that T-cell receptors transmit defined pN forces to their antigens for enhanced fidelity, Proc Natl Acad Sci U S A, 113 (2016) 5610-5615.
[86] Z. Wan, X. Chen, H. Chen, Q. Ji, Y. Chen, J. Wang, Y. Cao, F. Wang, J. Lou, Z. Tang, W. Liu, The activation of IgM- or isotype-switched IgG- and IgE-BCR exhibits distinct mechanical force sensitivity and threshold, Elife, 4 (2015).
[87] J.T. Groves, N. Ulman, S.G. Boxer, Micropatterning fluid lipid bilayers on solid supports, Science, 275 (1997) 651-653.
[88] T.D. Perez, W.J. Nelson, S.G. Boxer, L. Kam, E-cadherin tethered to micropatterned supported lipid bilayers as a model for cell adhesion, Langmuir, 21 (2005) 11963-11968.
[89] K.D. Mossman, G. Campi, J.T. Groves, M.L. Dustin, Altered TCR signaling from geometrically repatterned immunological synapses, Science, 310 (2005) 1191-1193.
[90] K. Salaita, P.M. Nair, R.S. Petit, R.M. Neve, D. Das, J.W. Gray, J.T. Groves, Restriction of receptor movement alters cellular response: physical force sensing by EphA2, Science, 327 (2010) 1380-1385.
[91] R.G. Moulick, D. Afanasenkau, S.E. Choi, J. Albers, W. Lange, V. Maybeck, T. Utesch, A. Offenhausser, Reconstitution of Fusion Proteins in Supported Lipid Bilayers for the Study of Cell Surface Receptor-Ligand Interactions in Cell-Cell Contact, Langmuir, 32 (2016) 3462-3469.
[92] T. Lohmuller, S. Triffo, G.P. O'Donoghue, Q. Xu, M.P. Coyle, J.T. Groves, Supported membranes embedded with fixed arrays of gold nanoparticles, Nano Lett, 11 (2011) 4912-4918.

[93] F. Pi, P. Dillard, R. Alameddine, E. Benard, A. Wahl, I. Ozerov, A. Charrier, L. Limozin, K. Sengupta, Size-Tunable Organic Nanodot Arrays: A Versatile Platform for Manipulating and Imaging Cells, Nano Letters, 15 (2015) 5178-5184.
[94] K.H. Biswas, K.L. Hartman, C.H. Yu, O.J. Harrison, H. Song, A.W. Smith, W.Y. Huang, W.C. Lin, Z. Guo, A. Padmanabhan, S.M. Troyanovsky, M.L. Dustin, L. Shapiro, B. Honig, R. Zaidel-Bar, J.T. Groves, E-cadherin junction formation involves an active kinetic nucleation process, Proc Natl Acad Sci U S A, 112 (2015) 10932-10937.
[95] K.H. Biswas, K.L. Hartman, R. Zaidel-Bar, J.T. Groves, Sustained alpha-catenin Activation at E-cadherin Junctions in the Absence of Mechanical Force, Biophys J, 111 (2016) 1044-1052.
[96] J.Y. Wong, J. Majewski, M. Seitz, C.K. Park, J.N. Israelachvili, G.S. Smith, Polymer-cushioned bilayers. I. A structural study of various preparation methods using neutron reflectometry, Biophys J, 77 (1999) 1445-1457.
[97] C. Delajon, T. Gutberlet, R. Steitz, H. Mohwald, R. Krastev, Formation of polyelectrolyte multilayer architectures with embedded DMPC studied in situ by neutron reflectometry, Langmuir, 21 (2005) 8509-8514.
[98] G. Decher, Fuzzy nanoassemblies: toward layered polymeric multicomposites, Science (Washington, D. C.), 277 (1997) 1232-1237.
[99] D. Beyer, G. Elender, W. Knoll, M. Kuehner, S. Maus, H. Ringsdorf, E. Sackmann, Influence of anchor lipids on the homogeneity and mobility of lipid bilayers on thin polymer films, Angew. Chem., Int. Ed. Engl., 35 (1996) 1682-1685.
[100] J. Spinke, J. Yang, H. Wolf, M. Liley, H. Ringsdorf, W. Knoll, Polymer-supported bilayer on a solid substrate, Biophys J, 63 (1992) 1667-1671.
[101] W.W. Shen, S.G. Boxer, W. Knoll, C.W. Frank, Polymer-supported lipid bilayers on benzophenone-modified substrates, Biomacromolecules, 2 (2001) 70-79.
[102] A. Kibrom, R.F. Roskamp, U. Jonas, B. Menges, W. Knoll, H. Paulsen, R.L.C. Naumann, Hydrogel-supported protein-tethered bilayer lipid membranes: a new approach toward polymer-supported lipid membranes, Soft Matter, 7 (2011) 237-246.
[103] M.K. Sharma, H. Jattani, M.L. Gilchrist, Bacteriorhodopsin conjugates as anchors for supported membranes, Bioconjugate Chem, 15 (2004) 942-947.

[104] E.S. Fried, J. Luchan, M.L. Gilchrist, Biodegradable, Tethered Lipid Bilayer-Microsphere Systems with Membrane-Integrated alpha-Helical Peptide Anchors, Langmuir, 32 (2016) 3470-3475.

[105] I.P. McCabe, M.B. Forstner, Polymer supported lipid bilayers, Open Journal of Biophysics, 3 (2013) 56-69.

[106] M.L. Wagner, L.K. Tamm, Tethered polymer-supported planar lipid bilayers for reconstitution of integral membrane proteins: Silane-polyethyleneglycol-lipid as a cushion and covalent linker, Biophysical Journal, 79 (2000) 1400-1414.

[107] C.A. Naumann, O. Prucker, T. Lehmann, J. Ruhe, W. Knoll, C.W. Frank, The polymer-supported phospholipid bilayer: Tethering as a new approach to substrate-membrane stabilization, Biomacromolecules, 3 (2002) 27-35.

[108] O. Purrucker, A. Fortig, R. Jordan, E. Sackmann, M. Tanaka, Control of frictional coupling of transmembrane cell receptors in model cell membranes with linear polymer spacers, Phys Rev Lett, 98 (2007).

[109] O. Prucker, C.A. Naumann, J. Rühe, W. Knoll, C.W. Frank, Photochemical attachment of polymer films to solid surfaces via monolayers of benzophenone derivatives, Journal of the American Chemical Society, 121 (1999) 8766-8770.

[110] B.A. Cornell, V.L. Braach-Maksvytis, L.G. King, P.D. Osman, B. Raguse, L. Wieczorek, R.J. Pace, A biosensor that uses ion-channel switches, Nature, 387 (1997) 580-583.

[111] S.M. Schiller, R. Naumann, K. Lovejoy, H. Kunz, W. Knoll, Archaea analogue thiolipids for tethered bilayer lipid membranes on ultrasmooth gold surfaces, Angew Chem Int Ed Engl, 42 (2003) 208-211.

[112] M.A. Deverall, E. Gindl, E.K. Sinner, H. Besir, J. Ruehe, M.J. Saxton, C.A. Naumann, Membrane lateral mobility obstructed by polymer-tethered lipids studied at the single molecule level, Biophysical Journal, 88 (2005) 1875-1886.

[113] Y. Kaizuka, J.T. Groves, Structure and dynamics of supported intermembrane junctions, Biophysical Journal, 86 (2004) 905-912.

[114] S.R. Tabaei, P. Jonsson, M. Branden, F. Hook, Self-assembly formation of multiple DNA-tethered lipid bilayers, J Struct Biol, 168 (2009) 200-206.

[115] M. Chung, R.D. Lowe, Y.H. Chan, P.V. Ganesan, S.G. Boxer, DNA-tethered membranes formed by giant vesicle rupture, J Struct Biol, 168 (2009) 190-199.

[116] D.H. Murray, L.K. Tamm, V. Kiessling, Supported double membranes, J Struct Biol, 168 (2009) 183-189.

[117] X. Han, A.S. Achalkumar, M.R. Cheetham, S.D. Connell, B.R. Johnson, R.J. Bushby, S.D. Evans, A self-assembly route for double bilayer lipid membrane formation, Chemphyschem, 11 (2010) 569-574.

[118] D.E. Minner, V.L. Herring, A.P. Siegel, A. Kimble-Hill, M.A. Johnson, C.A. Naumann, Iterative layer-by-layer assembly of polymer-tethered multi-bilayers using maleimide-thiol coupling chemistry, Soft Matter, 9 (2013) 9643-9650.

[119] L. Tayebi, Y. Ma, D. Vashaee, G. Chen, S.K. Sinha, A.N. Parikh, Long-range interlayer alignment of intralayer domains in stacked lipid bilayers, Nat Mater, 11 (2012) 1074-1080.

[120] H.E. Warriner, S.H. Idziak, N.L. Slack, P. Davidson, C.R. Safinya, Lamellar biogels: fluid-membrane-based hydrogels containing polymer lipids, Science, 271 (1996) 969-973.

[121] R.R. Bhat, B.N. Chaney, J. Rowley, A. Liebmann-Vinson, J. Genzer, Tailoring cell adhesion using surface-grafted polymer gradient assemblies, Adv Mater, 17 (2005) 2802-+.

[122] R.A. Segalman, Patterning with block copolymer thin films, Mat Sci Eng R, 48 (2005) 191-226.

[123] B.D. Gates, Q.B. Xu, M. Stewart, D. Ryan, C.G. Willson, G.M. Whitesides, New approaches to nanofabrication: Molding, printing, and other techniques, Chem Rev, 105 (2005) 1171-1196.

[124] T. Okazaki, T. Inaba, Y. Tatsu, R. Tero, T. Urisu, K. Morigaki, Polymerized lipid bilayers on a solid substrate: morphologies and obstruction of lateral diffusion, Langmuir, 25 (2009) 345-351.

[125] Y.H. Lin, D.E. Minner, V.L. Herring, C.A. Naumann, Physisorbed Polymer-Tethered Lipid Bilayer with Lipopolymer Gradient, Materials, 5 (2012) 2243-2257.

[126] O. Purrucker, A. Fortig, K. Ludtke, R. Jordan, M. Tanaka, Confinement of transmembrane cell receptors in tunable stripe micropatterns, Journal of the American Chemical Society, 127 (2005) 1258-1264.

[127] C.K. Yee, M.L. Amweg, A.N. Parikh, Direct photochemical patterning and refunctionalization of supported phospholipid bilayers, Journal of the American Chemical Society, 126 (2004) 13962-13972.

[128] K. Morigaki, K. Kiyosue, T. Taguchi, Micropatterned composite membranes of polymerized and fluid lipid bilayers, Langmuir, 20 (2004) 7729-7735.
[129] S. Waichman, F. Roder, C.P. Richter, O. Birkholz, J. Piehler, Diffusion and Interaction Dynamics of Individual Membrane Protein Complexes Confined in Micropatterned Polymer-Supported Membranes, Small, 9 (2013) 570-577.
[130] M.A. Deverall, S. Garg, K. Ludtke, R. Jordan, J. Ruhe, C.A. Naumann, Transbilayer coupling of obstructed lipid diffusion in polymer-tethered phospholipid bilayers, Soft Matter, 4 (2008) 1899-1908.
[131] E.B. Watkins, R.J. El-Khouri, C.E. Miller, B.G. Seaby, J. Majewski, C.M. Marques, T.L. Kuhl, Structure and Thermodynamics of Lipid Bilayers on Polyethylene Glycol Cushions: Fact and Fiction of PEG Cushioned Membranes, Langmuir, 27 (2011) 13618-13628.
[132] V. Kiessling, L.K. Tamm, Measuring distances in supported bilayers by fluorescence interference-contrast microscopy: Polymer supports and SNARE proteins, Biophysical Journal, 84 (2003) 408-418.
[133] H.L. Smith, M.S. Jablin, A. Vidyasagar, J. Saiz, E. Watkins, R. Toomey, A.J. Hurd, J. Majewski, Model Lipid Membranes on a Tunable Polymer Cushion, Phys Rev Lett, 102 (2009).
[134] P.G. Saffman, M. Delbruck, Brownian motion in biological membranes, Proc Natl Acad Sci U S A, 72 (1975) 3111-3113.
[135] O. Purrucker, A. Fortig, R. Jordan, M. Tanaka, Supported membranes with well-defined polymer tethers-incorporation of cell receptors, Chemphyschem, 5 (2004) 327-335.
[136] R. Bruinsma, M. Goulian, P. Pincus, Self-assembly of membrane junctions, Biophys J, 67 (1994) 746-750.
[137] D. Zuckerman, R. Bruinsma, Statistical mechanics of membrane adhesion by reversible molecular bonds, Phys Rev Lett, 74 (1995) 3900-3903.
[138] N. Gov, A.G. Zilman, S. Safran, Cytoskeleton confinement and tension of red blood cell membranes, Phys Rev Lett, 90 (2003) 228101.
[139] A. Nicolas, S.A. Safran, Elastic deformations of grafted layers with surface stress, Phys Rev E Stat Nonlin Soft Matter Phys, 69 (2004) 051902.
[140] N. Gov, S.A. Safran, Pinning of fluid membranes by periodic harmonic potentials, Phys Rev E Stat Nonlin Soft Matter Phys, 69 (2004) 011101.

[141] L. Zhang, S. Granick, Interleaflet Diffusion Coupling When Polymer Adsorbs onto One Sole Leaflet of a Supported Phospholipid Bilayer, Macromolecules, 40 (2007) 1366-1368.
[142] L. Zhang, S. Granick, Slaved diffusion in phospholipid bilayers, Proc Natl Acad Sci U S A, 102 (2005) 9118-9121.
[143] W. Rawicz, K.C. Olbrich, T. McIntosh, D. Needham, E. Evans, Effect of chain length and unsaturation on elasticity of lipid bilayers, Biophys J, 79 (2000) 328-339.
[144] D. Marsh, Elastic curvature constants of lipid monolayers and bilayers, Chem Phys Lipids, 144 (2006) 146-159.
[145] M. Seitz, C.K. Park, J.Y. Wong, J.N. Israelachvili, Long-range interaction forces between polymer-supported lipid bilayer membranes, Langmuir, 17 (2001) 4616-4626.
[146] M. Rovira-Bru, D.H. Thompson, I. Szleifer, Size and structure of spontaneously forming liposomes in lipid/PEG-lipid mixtures, Biophys J, 83 (2002) 2419-2439.
[147] D. Marsh, R. Bartucci, L. Sportelli, Lipid membranes with grafted polymers: physicochemical aspects, Biochim Biophys Acta, 1615 (2003) 33-59.
[148] W.C. Hwang, R.E. Waugh, Energy of dissociation of lipid bilayer from the membrane skeleton of red blood cells, Biophys J, 72 (1997) 2669-2678.
[149] R. Simson, E. Wallraff, J. Faix, J. Niewohner, G. Gerisch, E. Sackmann, Membrane bending modulus and adhesion energy of wild-type and mutant cells of Dictyostelium lacking talin or cortexillins, Biophys J, 74 (1998) 514-522.
[150] I. Bivas, V. Vitkova, M.D. Mitov, M. Winterhalter, R.G. Alargova, P. Meleard, P. Bothorel, Mechanical properties of lipid bilayers containing grafted lipids, Perspect. Supramol. Chem., 6 (2000) 207-219.
[151] A.P. Siegel, M.J. Murcia, M. Johnson, M. Reif, R. Jordan, J. Ruhe, C.A. Naumann, Compartmentalizing a lipid bilayer by tuning lateral stress in a physisorbed polymer-tethered membrane, Soft Matter, 6 (2010) 2723-2732.
[152] A.P. Siegel, N.F. Hussain, M. Johnson, C.A. Naumann, Metric between buckling structures and elastic properties in physisorbed polymer-tethered lipid monolayers, Soft Matter, 8 (2012) 5873-5880.
[153] R. Merkel, E. Sackmann, E. Evans, Molecular friction and epitactic coupling between monolayers in supported bilayers, J. Phys. (Paris), 50 (1989) 1535-1555.

[154] Y. Ge, Y.H. Lin, L.A. Lautscham, W.H. Goldmann, B. Fabry, C.A. Naumann, N-cadherin-functionalized polymer-tethered multi-bilayer: a cell surface-mimicking substrate to probe cellular mechanosensitivity, Soft Matter, 12 (2016) 8274-8284.
[155] P. Mascalchi, E. Haanappel, K. Carayon, S. Mazeres, L. Salome, Probing the influence of the particle in Single Particle Tracking measurements of lipid diffusion, Soft Matter, 8 (2012) 4462-4470.
[156] L.A. Lautscham, C.Y. Lin, V. Auernheimer, C.A. Naumann, W.H. Goldmann, B. Fabry, Biomembrane-mimicking lipid bilayer system as a mechanically tunable cell substrate, Biomaterials, 35 (2014) 3198-3207.
[157] D.E. Minner, P. Rauch, J. Kas, C.A. Naumann, Polymer-tethered lipid multi-bilayers: a biomembrane-mimicking cell substrate to probe cellular mechano-sensing, Soft Matter, 10 (2014) 1189-1198.
[158] H. Colognato, D.A. Winkelmann, P.D. Yurchenco, Laminin polymerization induces a receptor-cytoskeleton network, J Cell Biol, 145 (1999) 619-631.
[159] L. Woiterski, Claudepierre, T., Luxenhofer, R., Jordan, R., Kas, J., Stages of neuronal network formation, New Journal of Physics, 17 (2013).
[160] A. Engler, L. Bacakova, C. Newman, A. Hategan, M. Griffin, D. Discher, Substrate compliance versus ligand density in cell on gel responses, Biophys J, 86 (2004) 617-628.
[161] A.J. Engler, C. Carag-Krieger, C.P. Johnson, M. Raab, H.Y. Tang, D.W. Speicher, J.W. Sanger, J.M. Sanger, D.E. Discher, Embryonic cardiomyocytes beat best on a matrix with heart-like elasticity: scar-like rigidity inhibits beating, Journal of Cell Science, 121 (2008) 3794-3802.
[162] M.P. Sheetz, D.P. Felsenfeld, C.G. Galbraith, Cell migration: Regulation of force on extracellular-matrix-integrin complexes, Trends in Cell Biology, 8 (1998) 51-54.
[163] T. Shoaib, P.C. Nalam, Y. He, Y. Chen, R.M. Espinosa-Marzal, Assembly, Morphology, Diffusivity, and Indentation of Hydrogel-Supported Lipid Bilayers, Langmuir, 33 (2017) 7105-7117.
[164] B. Ladoux, W.J. Nelson, J. Yan, R.M. Mege, The mechanotransduction machinery at work at adherens junctions, Integr Biol (Camb), 7 (2015) 1109-1119.
[165] M. Miyazaki, M. Chiba, H. Eguchi, T. Ohki, S. Ishiwata, Cell-sized spherical confinement induces the spontaneous formation of contractile actomyosin rings in vitro, Nature Cell Biology, 17 (2015) 480-+.

[166] J. Lemiere, F. Valentino, C. Campillo, C. Sykes, How cellular membrane properties are affected by the actin cytoskeleton, Biochimie, 130 (2016) 33-40.
[167] M. Andreasson-Ochsner, G. Romano, M. Hakanson, M.L. Smith, D.E. Leckband, M. Textor, E. Reimhult, Single cell 3-D platform to study ligand mobility in cell-cell contact, Lab Chip, 11 (2011) 2876-2883.

Graphical Abstract

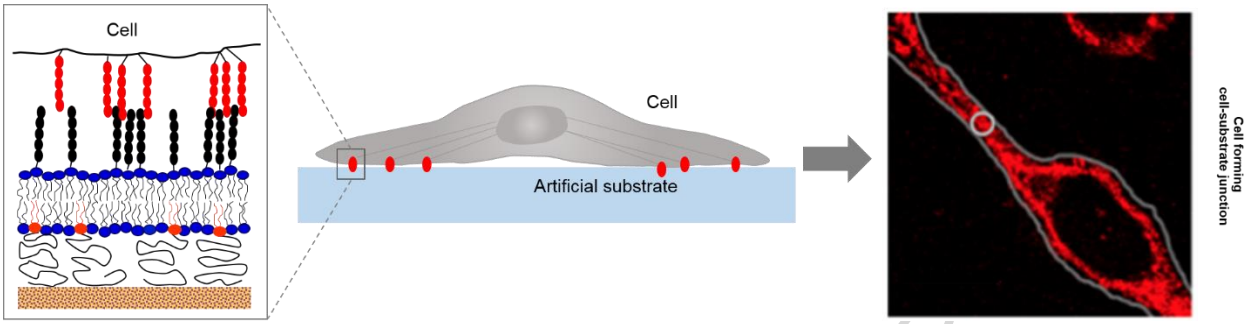

Highlights

Polymer-lipid hybrids are promising artificial cell substrates

Polymer-lipid hybrids allow formation/maturation of stable cell-substrate linkages

Cells spread and migrate on ligand-functionalized polymer-tethered lipid bilayers

Tunable polymer-tethered lipid bilayers enable studies of cellular mechanosensitivity